



ISLAMIC UNIVERSITY OF TECHNOLOGY
ORGANIZATION OF ISLAMIC COOPERATION



Harvesting low-frequency acoustic energy using multiple PZT films and complex design variations of the Helmholtz resonator

A THESIS SUBMITTED TO THE ACADEMIC FACULTY IN PARTIAL FULFILLMENT
OF THE REQUIREMENT FOR THE DEGREE OF

BACHELOR OF SCIENCE
IN
MECHANICAL ENGINEERING

AUTHORED BY,

Nafis Md. M. Islam
Student ID: 180011123

Md. Saifur Rahman
Student ID: 180011210

Supervised By

Prof. Dr. Md. Anayet Ullah Patwari
Head, Department of Mechanical and Production Engineering
Islamic University of Technology
Board Bazar, Gazipur
Bangladesh

DEPARTMENT OF MECHANICAL AND PRODUCTION ENGINEERING

ISLAMIC UNIVERSITY OF TECHNOLOGY

CANDIDATE'S DECLARATION

It is hereby declared that their thesis or any part of it has not been submitted elsewhere for the award of any degree or diploma.

Signature of Candidates

Nafis Md. M. Islam.
28.05.23

Nafis Md. M. Islam

Md. Saifur Rahman

Md. Saifur Rahman

Department of Mechanical and Production Engineering
Islamic University of Technology
Board Bazar, Gazipur
Bangladesh

Signature of Supervisor

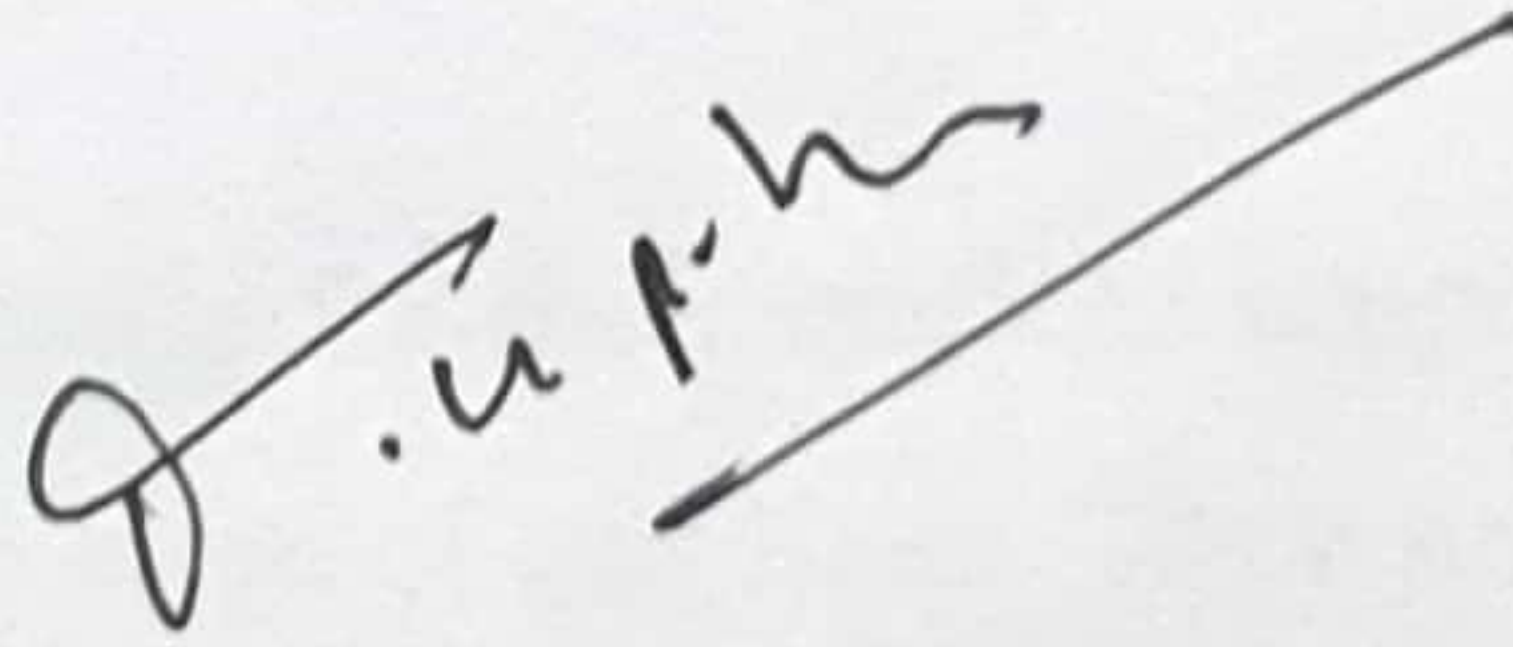
Prof. Dr. Md. Anayet Ullah Patwari

Prof. Dr. Md. Anayet Ullah Patwari
Head, Department of Mechanical and Production Engineering
Islamic University of Technology
Board Bazar, Gazipur
Bangladesh

CERTIFICATE OF RESEARCH

The thesis titled “**Harvesting low-frequency acoustic energy using multiple PZT films and complex design variations of the Helmholtz resonator**” submitted has been accepted as satisfactory in partial fulfillment of the requirements for the degree of Bachelor of Science in Mechanical Engineering on May 2023.

Supervisor



Prof. Dr. Md. Anayet Ullah Patwari

Head, Department of Mechanical and Production Engineering
Islamic University of Technology
Board Bazar, Gazipur
Bangladesh

ACKNOWLEDGEMENT

At the beginning of this study, we would like to state our sincerest gratitude to the Almighty for the fortune of good health and scope to conduct this experimental research. Indeed, all praises are to Him, and only His guidance can show us the true path to excellence.

Our utmost thanks to our supervisor Prof. Dr. Md. Anayet Ullah Patwari, Head, Department of MPE, Islamic University of Technology (OIC), for his tireless efforts, directions, and innovative ideas, which have shaped this research. We are both thankful and humbled by his support and motivation. Without him, this research would not be successful.

We thank the Department of Mechanical and Production Engineering (MPE) for providing us with all sorts of technical facilities. The labs, experimental setups, and equipment have been critical components of this study. Henceforth, all academic personnel related to these facilities have a part in the success and betterment that this study might provide to society.

Lastly, to our family, we have all the gratitude for their endless support, motivation, encouragement, and struggles that went into bringing us to this stage of our lives. They hold the most extensive credit for our success, and it was impossible for us to conduct this without them.

ABSTRACT

Acoustic energy harvesting is a form of Low-frequency energy harvesting and is a highly complicated process. It has been one of the most popular fields of research for the scientists of energy harvesting. It is partly because it utilizes low-frequency energy, a very potential and available source. But mainly because these types of energy can be harvested using minimal components with very low-budget setups, which makes it cost-effective and practical. The physical characteristics of piezoelectric materials can be utilized to extract energy from low-frequency acoustic or vibration-based waves. This means most of the vibrations and waves that are considered to be polluting and unnecessary can be converted into a usable form of energy to not only suppress the effects but also gain useful outcomes. If low-frequency energy can be utilized through a resonator, it can create excitement on various forms of PZT sensors to gain voltage as an output. In this study, experiments have been conducted on acoustic energy harvesting from low-frequency sound sources using Helmholtz Resonator with multiple PZT film configurations and designing complex shapes of resonator inlets. This study also focuses on the changes in outcomes for changing the orientations of the PZT films, the number of the PZT films, and so on. Based on the results obtained from the experiment, it was clear that a double film configuration in a parallel orientation is better for the purpose. The best outcomes were obtained by increasing the number of films to three and in a parallel configuration. However, changes in resonator inlets did not show any significant development in the output. Hence, it was concluded that the existing design was better suited for efficient energy harvesting. The experiment was done under the condition of 500mV and 1000mV. These modified Helmholtz Resonator designs and multiple film configurations can be used to power up low-power-consuming devices and are extensively applicable for noise reduction in big cities and industrial areas.

Keywords: low-frequency power, acoustic energy harvesting, Helmholtz Resonator, PZT materials, complex 3D designs.

Table of Contents

List of Figures.....	6
List of Tables.....	7
Chapter One: Introduction.....	8
1.1 Introduction.....	8
1.2 Fundamentals of Helmholtz Resonator.....	9
1.2.1 Different Types of Piezoelectric Sensors.....	11
1.3 Objectives.....	14
1.4 Thesis Organization.....	14
Chapter Two: Literature Review.....	15
2.1 Energy Harvesting Techniques.....	15
2.2 Acoustic Energy Harvesting.....	16
2.3 Helmholtz Resonator.....	17
2.4 PZT Films.....	18
Chapter Three: Research Methodology.....	20
3.1 Methodology.....	20
3.2 Geometry.....	21
3.2.1 Single Unit of Helmholtz Resonator.....	22
3.2.2 Array Design of Helmholtz Resonator.....	23
3.3 3D Printing Machine.....	24
3.3.1 3D Model.....	25
3.3.2 Modified 3D Models.....	26
3.3.3 Orientation of the Films.....	27
3.3.4 Orientation of Increased Films.....	29
3.4 PZT Film Description.....	30
3.5 Sound Source.....	34
3.6 Experimental Details.....	35
3.7 Boundary Conditions.....	37
Chapter Four: Results and Discussions.....	38
4.1 Experimental Results.....	38
4.1.1 Single Film vs. Perpendicular Double Films.....	38
4.1.2 Parallel Double Films vs. Perpendicular Double Films.....	40
4.2 Comparative Results.....	42
4.2.1 Single and Double Films vs. Perpendicular Films.....	42
4.2.2 Single and Double Films vs. Triple Films.....	44
4.2.3 Triple films in Original vs. Converging vs. Diverging Inlets.....	46
Chapter Five: Conclusion and Future Scopes.....	49
5.1 Summary.....	49
5.2 Future Scopes.....	49
5.3 Conclusion.....	50
Chapter Six: References.....	51

List of Figures

Figure 1.1: Helmholtz Resonator [1]	9
Figure 1.2: Design of Bottle Helmholtz Resonator [2]	10
Figure 1.3: Design of Pipe Helmholtz Resonator [3]	11
Figure 1.4: Polarization process of PZT and stress-induced phase transition in PZT.[4]	13
Figure 1.5: Design of PZT thin-film acoustic actuators [5]	13
Figure 1.6: Schematic structure of PVDF foil piezoelectric transducer [6]	14
Figure 1.7: Schematic structure of piezoelectric accelerometer transducer [7]	14
Figure 3.1: The architecture of the study	21
Figure 3.2: Front and Bottom view of the prototype along with dimensions [1]	22
Figure 3.3: Array design of the prototype for the noise barrier.....	23
Figure 3.4: 3D printing machine.....	24
Figure 3.5: Assembled and disassembled views of the prototype.....	25
Figure 3.6: Converging and diverging designs for the new inlet	26
Figure 3.7: Film orientation of the previous study.[1]	27
Figure 3.8: Film orientation of the new prototype.....	28
Figure 3.9: Triple film concept using the Helmholtz Resonator	29
Figure 3.10: PZT film without resonating mass	30
Figure 3.11: Speakers (Havit HV-SK473) used in the experiment	34
Figure 3.12: Physical demonstration of the experimental Setup	35
Figure 3.13: Flow diagram of the experimental setup.....	36
Figure 4.1: Output Voltage vs. Input Frequency at 500mV fixed input voltage	38
Figure 4.2: Output Voltage vs. Input Frequency at 1000mV fixed input voltage.....	39
Figure 4.3: Output Voltage vs. Input Frequency at 500mV fixed input voltage	40
Figure 4.4: Output Voltage vs. Input Frequency at 1000mV fixed input voltage.....	41
Figure 4.5: Comparison of output at 500mV fixed input voltage	42
Figure 4.6: Comparison of output at 1000mV fixed input voltage	43
Figure 4.7: Data comparison for triple films at 1000mV fixed input voltage	44
Figure 4.8: Comparison of output for triple films at 1000mV fixed input voltage	44
Figure 4.9: Data comparison for triple films at 500mV fixed input voltage	45
Figure 4.10: Comparison of output for triple films at 500mV fixed input voltage	45
Figure 4.11: Data comparison for triple films at 500mV fixed input voltage	46
Figure 4.12. Comparison of output for different inlet designs at 500mV fixed input voltage	47
Figure 4.13: Data comparison for triple films at 1000mV fixed input voltage	47
Figure 4.14: Comparison of output for different inlet designs at 1000mV fixed input voltage.....	48

List of Tables

Table 3.1	31
Table 3.2	32
Table 3.3	33
Table 3.4	34
Table 3.5	37

Chapter One

Introduction

1.1 Introduction

Acoustic sound waves are mechanical waves with energy produced by a wide range of noise sources. When the sound wave is unwanted, it's referred to as noise. The typical noise sources are aircraft, vehicles, high-speed trains, power stations, loudspeakers, and expressways. The conversion of mechanical vibration to electrical energy can be performed using piezoelectric, electromagnetic, and electrostatic generators. In this study, the focus has been given mainly to piezoelectric transduction. Piezoelectric (PZT) is a sophisticated replacement for batteries that can instantly generate energy. A lot of research has been done on this topic. The majority of the studies produced power/voltage at a high frequency, which is used in military and government communication systems, aviation, and over-the-horizon radar systems. However, the need for acoustic energy harvested from low frequencies present in our daily life, such as traffic, TVs, aircraft, metro rail, industries, and many other sound sources, is discovered and investigated in this work. In addition, all previous studies produced power using a single/double piezoelectric beam, and the use of modified resonator designs has not been investigated. As a result, the primary goal of this study is to figure out a new method for extracting energy from low-frequency sound waves that employ multiple piezoelectric beams with a honeycomb structure Helmholtz resonator while optimizing the shapes to see the changes in outcome. Due to the use of multiple PZTs, this method can hopefully increase the amount of energy harvested. A honeycomb structure Helmholtz resonator is fabricated after designing an acceptable PZT setup to amplify the voltage produced by the PZT setup. Inlet structures for more efficient operation will also be generated based on the study results.

1.2 Fundamentals of Helmholtz Resonator

The Helmholtz resonator is a straightforward acoustic device with a rigid-walled chamber of volume V that is filled with air and a neck of section S and length L that connects the cavity to the outside world. The system's air is under atmospheric pressure. The air filling the neck begins to flow back and forth upon a sufficient brief outside pressure stimulation, dampening out in due course. A mechanical vibrating system with one degree of freedom is able to approximate and characterize the behavior of the air.

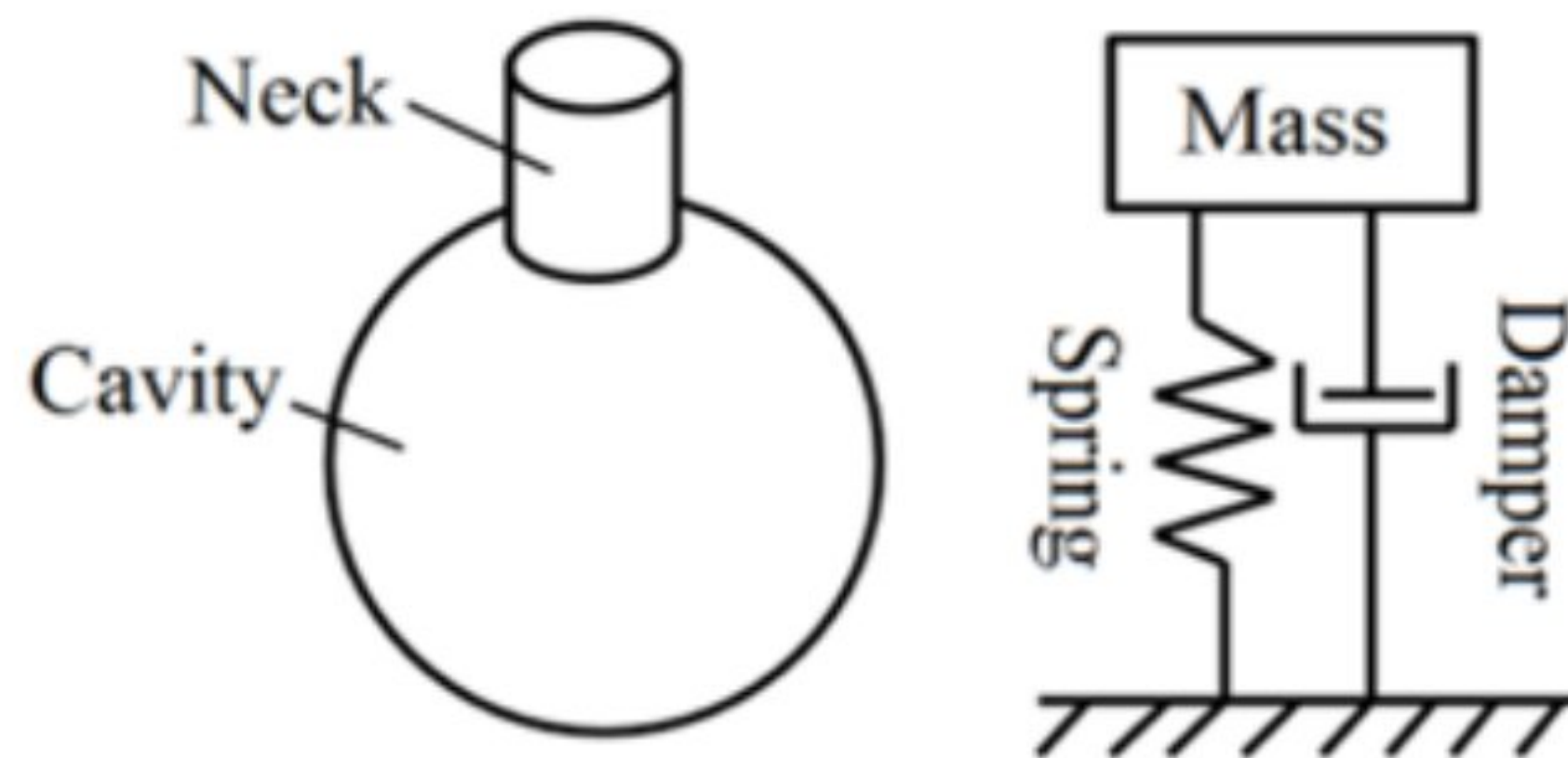


Figure 1.1: Helmholtz Resonator [1]

The dimensions of the cavity and neck are significantly less than the acoustic wavelength at the fundamental natural frequency. For hundreds of years, people have used these phenomena to create musical instruments. Recently, they have been utilized for noise control purposes in the automobile sector, for the design of mufflers, for habitational acoustics, subwoofers, music hall acoustics, or sports arenas to improve sound absorption at low frequencies, among other things. The Helmholtz resonator may be viewed as an amplifier now at resonance.

Different types of Helmholtz resonators include

- Bottle resonators.
- Pipe resonators.
- Spherical resonators.

Some examples are discussed below:

Bottle Resonator

A straightforward and often-used design is the bottle resonator. It comprises a more extensive body and a narrower neck on a bottle-shaped container. The body operates as the resonating chamber, while the neck serves as the intake for sound waves. The body volume, neck length, and neck diameter all affect the bottle resonator's resonance frequency.

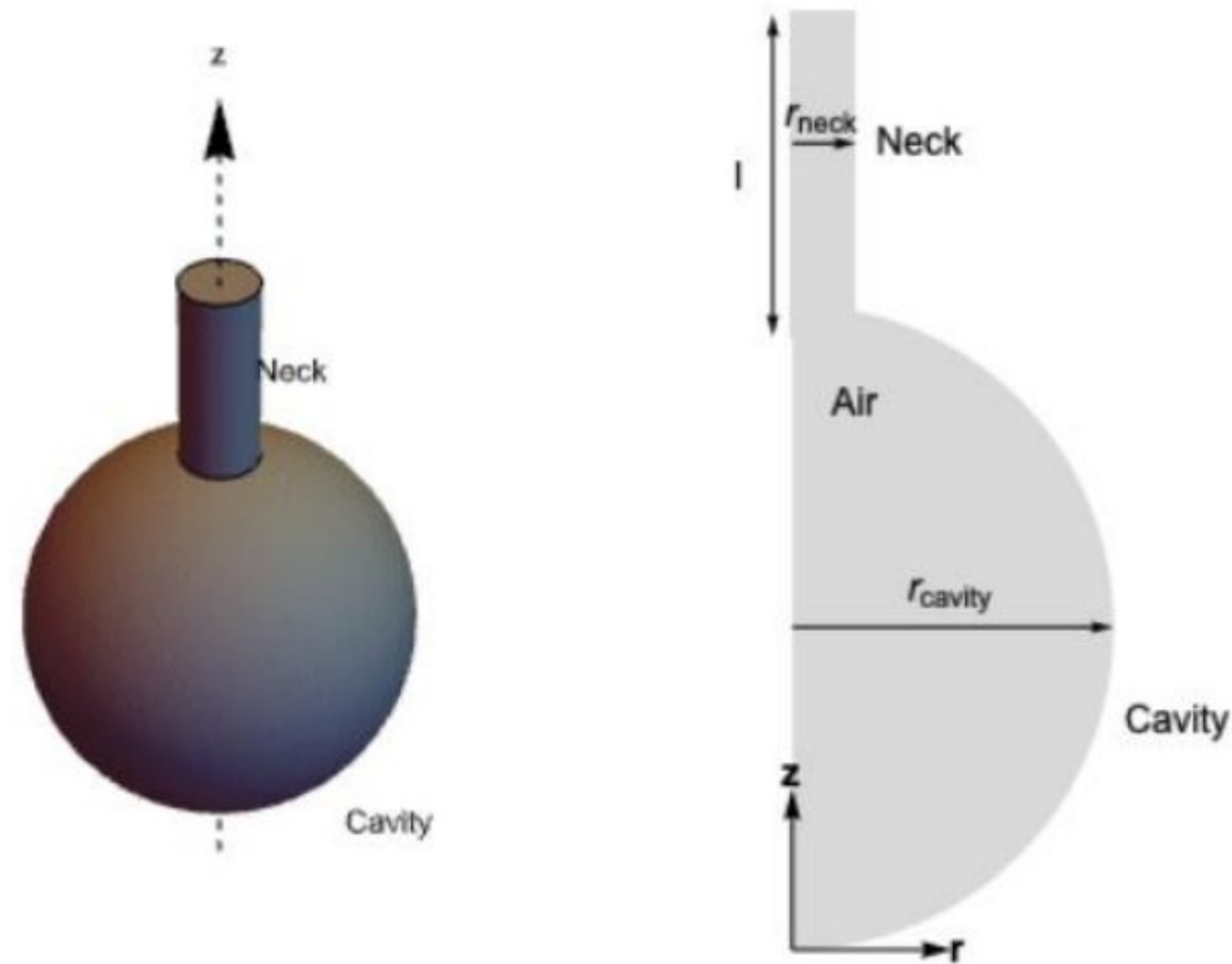


Figure 1.2: Design of Bottle Helmholtz Resonator [2]

Pipe Resonator

The resonating chamber of the pipe resonator, also called a tubular resonator, is a cylindrical pipe. The pipe has an open end on one side and a closed or open end on the other. The resonance frequency depends on the pipe's length and diameter. Exhaust systems and instruments for music, like organ pipes, frequently employ pipe resonators.

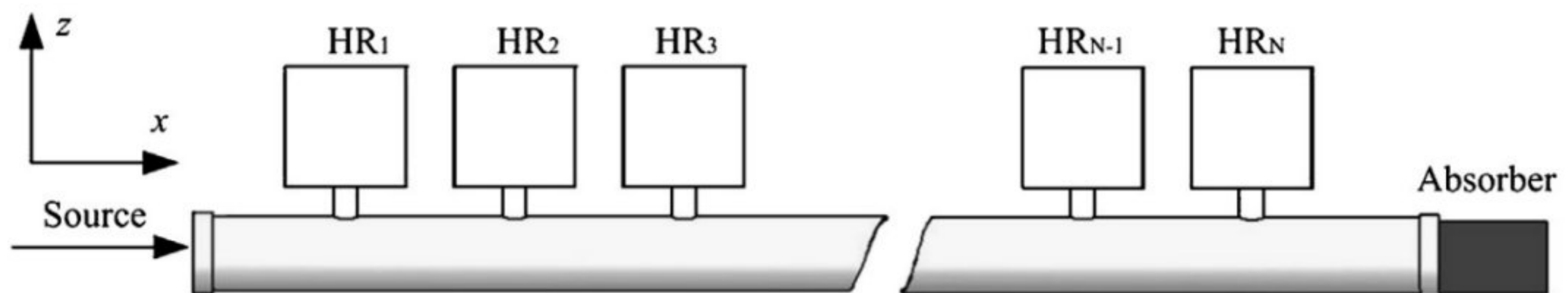


Figure 1.3: Design of Pipe Helmholtz Resonator [3].

1.2.1 Different Types of Piezoelectric Sensors

The piezoelectric sensors can be classified into four types: [5]

- Piezoelectric force sensor
- Piezoelectric pressure sensor
- Piezoelectric acceleration sensor
- Polymer pressure sensor

Some of the examples are discussed below:

PZT

Even in the absence of mechanical force, PZT has a net positive charge in every cell unit due to its lack of central symmetry. The titanium ion's location within the unit cell alters when stress is applied, which causes the establishment of an electrochemical polarity. The unit cell becomes an electric dipole as a result of this change.

Inorganic materials need to be poled by being exposed to a strong electric field at a high temperature in order to produce piezoelectricity. Regardless of an applied electric field, PZT may have its inner dipoles redirected by a field of electricity outside, producing a residue polarization.

PZT has better sensitivity and a higher operating temperature range when compared to previously identified metallic oxide-based piezoelectric materials. Additionally, PZT is chemically stable, physically durable, and very easy to produce. It is widely sought-after for use in biodevices due to its exceptional electro-mechanical capabilities, notably its huge piezoelectric charge constant.[4]

PZT is piezoelectric porcelain with high piezoelectric constants that are frequently utilized as sensors and actuators. To do this, research is conducted to create PZT thin-film micro-sensors and actuators.[5]

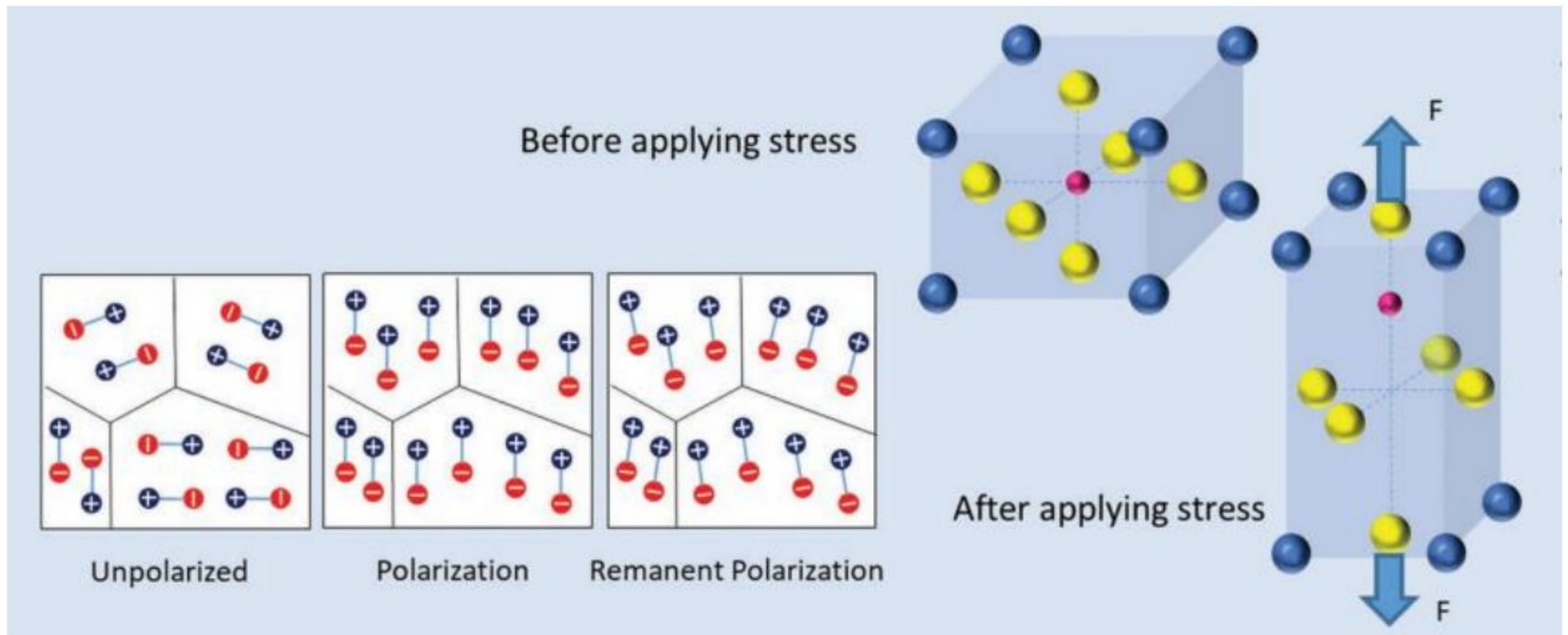


Figure 1.4: Polarization process of PZT and stress-induced phase transition in PZT.[4]

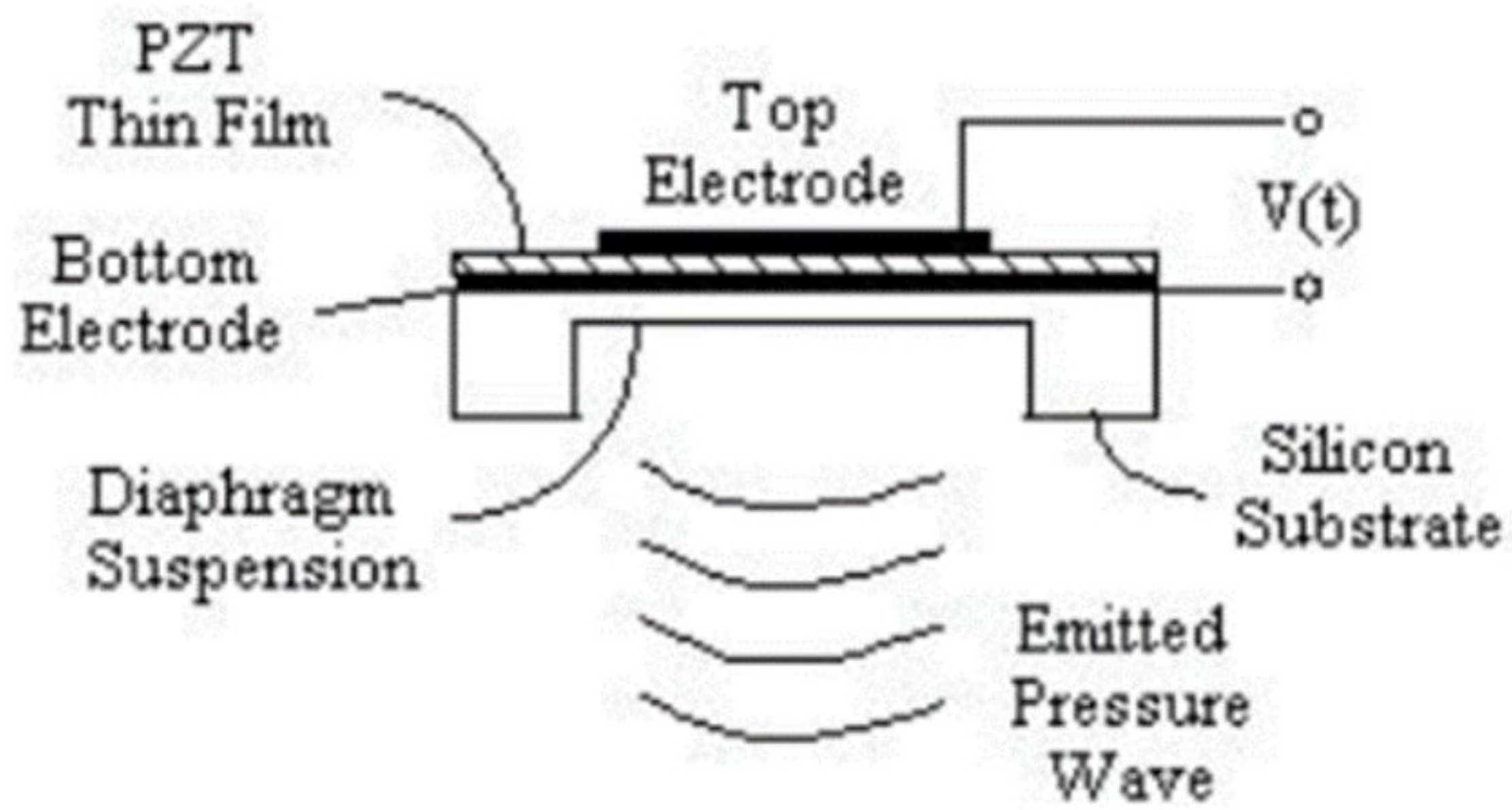


Figure 1.5: Design of PZT thin-film acoustic actuators.[6]

PVDF

A type of polymer piezoelectric material with a piezoelectric action is Polyvinylidene Fluoride (PVDF). Since it is a polymer, it is light and comfortable, making it ideal for numerous uses, including capturing energy from wind, rain, tides, and other natural phenomena. PVDF is inexpensive and can be cut to any size and shape when heated to lower temperatures.[6]

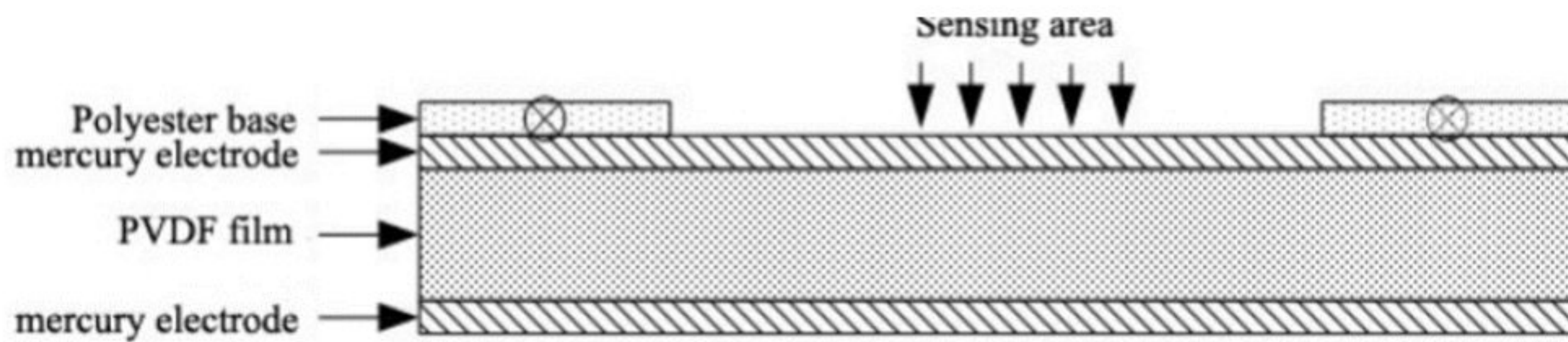


Figure 1.6: Schematic structure of PVDF foil piezoelectric transducer.[7]

Piezoelectric Accelerometer Sensor

The piezoelectric accelerometer sensor's structural design is shown in the picture. Two piezoelectric sheets typically make up a piezoelectric element. In either case, a piece of metal is sandwiched between two piezoelectric sheets, the lead is welded to the metal sheet, and the other lead at the output end is directly linked to the sensor base. The output lead is then coated with silver layers on both surfaces of the piezoelectric sheet. A strong spring, a bolt, or a nut is used to preload a mass with a higher specific gravity after it has been put on the piezoelectric sheet. The entire component is mounted inside a sturdy metal casing. [8]

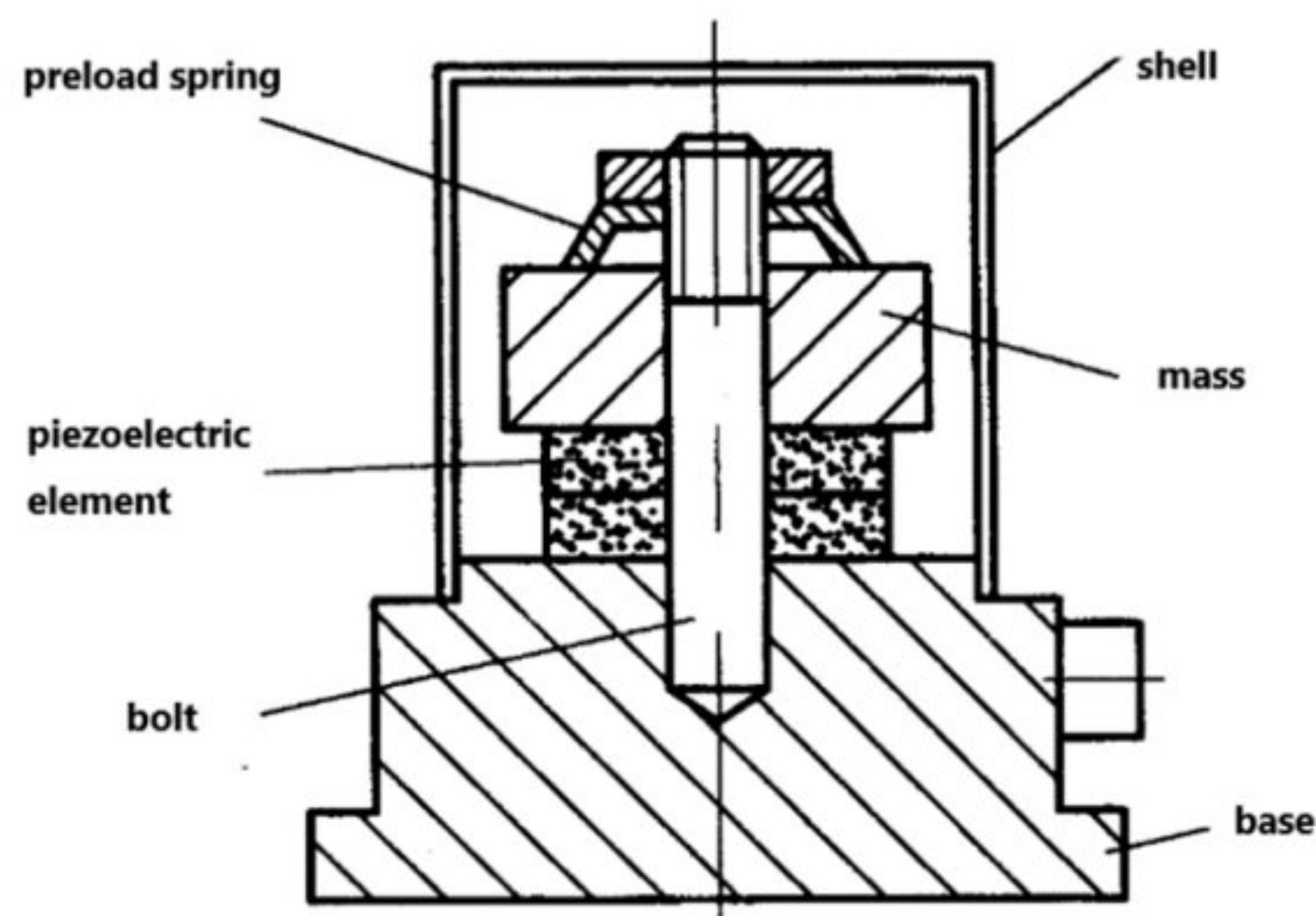


Figure 1.7: Schematic structure of piezoelectric accelerometer transducer.[8]

1.3 Objectives

The long-term goal of this project is to attain energy by reducing unwanted noise from surroundings. Specific objectives are listed below:

- To develop the existing technology of vibration-based energy harvesting further by using an increased number of PZT films.
- To assess the potential of readily available piezoelectric materials.
- To develop and produce more efficient Helmholtz Resonator inlet designs.
- To formulate a comparative study with previous works.

Expected Outcomes

- Changing the orientation of the films to perpendicular may not show significant improvement in results.
- Increasing the number of PZT films could provide a breakthrough in output voltage.
- Developing an innovative inlet design could show promising results, but the designs must be tested for further betterment.

1.4 Thesis Organization

This research starts with an introduction in **Chapter One** that gives foundation knowledge on acoustic energy harvesting and is followed by a review of different techniques for obtaining energy from sources of low-frequency sound and vibration. **Chapter Two** contains a thorough literature analysis of prior investigations along with the process for collecting acoustic energy using different methods, PZT films, and the Helmholtz resonator. **Chapter Three** has a detailed explanation of our work process and the design of multiple PZTs and the Helmholtz Resonator. Different inlet design configurations are also offered. This chapter presents an experimental evaluation of the different design setups and noise barriers for acoustic energy harvesting from our thesis. **Chapter Four** demonstrates the viability and benefit of the proposed noise barrier system based on the results and analysis from the trials conducted in this study. At the beginning of **Chapter Five**, a summary of the findings is given with a summary of the outputs. Later on, the conclusion drawn by the authors based on the results is discussed. It also dictates the future scope and potential of the study. **Chapter Six** provides all the necessary references and links to help navigate the easy study of this research study.

Chapter Two

Literature Review

The literature review conducts a critical analysis of the corpus of knowledge and academic works on energy harvesting using multiple PZT film configurations in Helmholtz resonators. In order to lay the groundwork for this study, it seeks to identify relevant themes, information gaps, and theoretical frameworks. The present state of research in the area is thoroughly summarized in this section.

2.1 Literature Review on Energy Harvesting Techniques

Anayet et al. [1] employed piezoelectric material's physical properties to capture energy from vibration-based waves. They employed a Helmholtz resonator with PZT films. It was suggested that an array of devices be utilized in metro tracks to lessen noise. Zhang et al. [9] introduced a new shock absorber to collect the waste of suspension energy from moving vehicles for use in extended electric vehicles. Abbas et al. [10] examined the energy-collecting methods that are currently employed for bridge and road construction for various uses. Xingtian et al. [11] established a portable electromagnetic energy harvesting design that utilizes mechanical transmission to transform railroad vibrations into electricity. The proposed energy harvester was found to be efficient in testing, with a 55.5% efficiency. The electrostatic mechanism suggested by Granstrom et al. [12] is the best match for MEMS applications and does not require smart material. However, this type of charger involves an external voltage source, such as a battery, and has mechanical limitations. Abdelmoula et al. [13] studied a low-frequency Zigzag energy harvester with torsion bending properties and confirmed that the proposed torsion-dominant mode provided a higher harvested power level while lowering the operating frequency by half. Özge et al. [14] demonstrated a brand-new vibration-based electromagnetic energy harvester that can extract energy from low-frequency external vibrations between 1 and 10 Hz utilizing a mechanical frequency up-conversion technique. Scavenging vibrational energy using piezoelectric materials was brought out by Steven et al. [15]. This article reviews the existing research on power harvesting with an eye toward creating totally self-powered gadgets. Hansen et al. [16] proposed a device with the capability of scavenging hybrid energy by using a PVDF nanogenerator made of nanofibers. Ovejas et al. [17] analyzed the usage of PZT films in wind energy harvesting by utilizing laminar and turbulent flow. Fondevilla et al. [18] proposed a design to harvest energy from slow oscillating movements of ambient wind with the help of a non-resonant energy harvester.

2.2 Literature Review on Acoustic Energy Harvesting

Kim et al. [19] constructed an acoustic energy scavenger to use large amplitude acoustic waves, which formed in response to the air flowing through the entrance of the HR. At rotating frequencies of 7–13,5 Hz, an output power of 83.5–825 μ W is gained. Mickaël et al. [20] attempted to increase the power gain in high-frequency acoustic energy harvesting. Luo et al. [6] talked about acoustic energy harvesting (AEH), which transforms environmental acoustic waves into electricity using a resonator or a transducer, which has now become viable with the fast technological development of autonomous microelectromechanical systems (MEMS). Guan et al. [21] developed a piezoelectric system for gaining rotational energy, for example, generators built into the interior surface of the tires of the vehicle. The frequent deformations of the piezoelectric elements are transported to electricity while the energy collector rotates. Stephen et al. [22] reported preliminary findings regarding creating an aero-acoustic energy harvester using micromachines. The design, construction, and characterization of a microfabricated acoustic energy extractor prototype using lumped elements were shown. Yuan et al. [23] suggested increasing the output power of acoustic energy gathering and introducing a unique design for harvesting acoustic energy. The suggested high device comprises an HR with an unfixed bottom that works well with low-frequency sound waves. Due to the low sound strength, Yuan et al. [24] transformed acoustic energy into electric energy in a Helmholtz resonator using a PVDF film in the electricity generator module and sound pressure. Liyang-Yu et al.'s [25] research was centered on developing a sound energy harvester that combined piezoelectric material with a sonic crystal. The localization of the sound waves within the cavity's resonance frequency was made possible by inserting a point defect into the sonic crystal. Yuan et al. [26] studied the importance of acoustic energy harvesting and its future scopes as a potential energy-harvesting topic of research. Pillai et al. [27] proposed the use of piezoelectric technology to harvest thermoacoustic energy and reviewed the results. Williams et al. [28] used acoustic vibration to generate and supply power to microelectronics using piezoelectric materials. Khan et al. [29] developed a Helmholtz resonator based on electromagnetic principles to harvest acoustic energy of different sound pressure levels. Their study explored the outputs of forward and reverse frequency sweep simultaneously.

2.3 Literature Review on Helmholtz Resonator

Glynne-Jones et al. [30] detailed the creation of microgenerators that can transform vibrational energy from the environment into electric power for use in supplying smart sensor systems. Marco et al. [31] illustrated a multi-frequency mechano-electrical piezoelectric inverter designed to supply autonomous sensors with electricity from ambient vibrations. Vatansever et al. [32] studied renewable energy production from raindrops and wind speeds. Ceramic-based piezoelectric fiber composite structures (PFCs) and polymer-based piezoelectric strips, PVDF (Polyvinylidene fluoride), were used to generate a voltage from these natural phenomena in driving small devices. Conclusions were drawn after running different experiments on both piezoelectric materials and varying parameters such as droplet weight, releasing height, and wind speed. Afterward, Li et al. [33] used PVDF cantilever beams to monitor the 58 cm tube resonator in two different configurations: aligned and zigzag. In comparison to the aligned design, the zigzag structure showed a substantial increase in voltage and power. The zigzag configuration provides a wider path for acoustic air particle motion, resulting in a higher amplification ratio. Sung-Eun et al. [34] suggested an extensible PVDF (polyvinylidene fluoride) cantilever that can automatically change its resonance frequency and retain the switched frequency without consuming energy. He established that the suggested energy harvester could alter its resonance frequency without an additional energy source in a brief amount of time. Orrego et al. [35] developed a novel wind energy harvester by self-sustaining oscillations of a flexible piezoelectric membrane fixed in an inverted orientation. Helios Vocca et al. [36] proposed a vibration harvesting system using bi-stable oscillators to model nonlinear piezoelectric harvesters to explore the perspective of noise-driven dynamics. Li et al. [37] used PZT beams as a piezoelectric material in their tube resonator. Two separate-length tube resonators were built to check the output voltage of the piezoelectric material plates. Li et al. [38] presented and investigated a system for collecting acoustic energy at low audible frequencies both experimentally and computationally. Due to the PZT plates' interference with air particle motion, the maximum number of PZT plates needed to maximize voltage and power is constrained. Hossein et al. [39] clarified the suitability of harvesting mechanical energy from vehicle strain and stress produced on highways. They conducted experiments to see whether piezoelectric materials could be used to harvest energy from asphalt pavements. Zhao et al. [40] used a double-tube Helmholtz resonator and discussed ways to efficiently harvest acoustic energy with their nanogenerator.

2.4 Literature Review on PZT Films

Liu et al. [41] proposed the creation of an electro-mechanical Helmholtz resonator (EMHR) with multiple degrees of freedom (MDOF) that can be tuned. The absorption coefficient of two EMHR layouts with various resistive, inductive shunts is measured using the two-microphone approach. Liu et al. [42] investigated the development of an acoustic energy harvesting system based on an electro-mechanical Helmholtz resonator (EMHR), which usually consists of a cavity, orifice, and piezoelectric diaphragm. In the case of an incident SPL of approximately 160 dB, the power output can be up to nearly 30 mW, which is sufficient to power many low-power electrical appliances. Zhou et al. [43] demonstrated an acoustic energy harvester in a bistable state with a flat plate that is excited to vibrate. A high voltage output was produced for a specific sound pressure level (SPL) when reaching a coherence resonance. Noh et al. [44] suggested a piezoelectric cantilever incorporated into the HR. To enhance the efficiency of harvesting energy, the mechanical resonance of the piezoelectric cantilever was consistent with the acoustic resonance of the HR. Although existing initiatives have partially addressed the problems of noise pollution and energy waste, some aspects of (MR/Industries/Airport) noise still needs to be resolved. Zhang et al. [45] proposed a kinetic energy recovery device to capture the energy wasted by vehicles going through a road tunnel. The results of the investigation were implicated by Noh et al. [43] for both noise mitigation and acoustic energy harvesting applications. A piezoelectric cantilever was incorporated into the study's resonator to improve energy harvesting effectiveness. Lupea et al.'s [46] compared the acoustic modal analysis with natural frequencies from different techniques, revealing good agreement, suggesting the possibility of simulating and optimizing increasingly complicated systems. Roundy et al. [47] proposed different designs and optimized models of resonators based on the bending of two-layer elements. Zhongyu et al. [48] proposed different techniques for tuning an acoustic resonator and the effect of using a mistuned resonator in acoustic energy harvesting. They also discussed the effects internal resistance has on energy dissipation. Smits et al. [49] proposed piezoelectric cantilever bimorphs and dynamic admittance of their matrix.

In this work, we put up a proposal to address the issues stated previously regarding noise pollution around (MR/Industries/Airport). We propose the installation of a noise barrier that, in addition to lowering noise levels, also captures alternative acoustic energy that can be used for generating power. Two essential elements are included in the suggested noise barrier: a high-reaction (HR) device and a material called piezoelectric (PZT) film. The noise barrier may generate power and effectively lower noise levels by combining various technologies. Due to its dual functioning, which captures the power that would otherwise be wasted, noise pollution may be addressed sustainably. There are a number of useful uses for the installation of this sound blocker and energy production system near (MR/Industries/Airport). For instance, the electricity produced may be utilized to run important infrastructure, like runway lights at airports, metro train operations monitoring systems, tiny electronic gadgets in industries, and upkeep tools. This article offers an all-encompassing plan to reduce noise pollution and use energy sources that are renewable in (MR/Industries/Airport) environments. By putting in place the suggested noise barrier, we can solve noise issues while also helping to create a healthier and more energy-efficient environment.

Chapter Three

Research Methodology

3.1 Methodology

The methodology behind this study was to extend the research work done by Md. Anayet et al. [1] where they were using single and double PZT film configurations for harvesting low-frequency vibrations. As mentioned in the literature review above, they have found significantly high output voltages by implementing two films in a parallel configuration embedded inside a Helmholtz resonator. This study has aimed to conduct a comparative analysis of that result using multiple PZT films (more than two) on different configurations and modified resonator inlet designs. Additionally, the possibility of a further increase in output is to be analyzed through this study.

At first, the existing results, based on the study of Md. Anayet et al. [1] will be tested again by conducting the experiment in the applied mechanics lab. Afterward, different orientations will be tested, including the perpendicular orientation discussed before, using the same dual film setups to understand the changes in output voltage for orientation change and a probable increase. Afterward, new configurations are to be investigated with a higher number of PZT films for increased output. Finally, at least two more designs will be developed for the inlet part of the resonator, and a comparative experimental study will be done among the obtained results.

To properly understand the methodology of this study, it is necessary to comprehend the architecture of the process of converting low-frequency energy into voltage. To help understand that better, a flow diagram has been added in **Figure 3.1**. The low-frequency energy from the speaker converges in the resonator inlet for its special shape and enters the resonator through the pore. This energy then resonates inside the resonator and then creates excitement in the PZT materials. The material then gives an output in the form of voltage, which is observed and measured through the oscilloscope. Increasing or decreasing the number of films, changing the geometrical orientation, complex resonator designs, and inlets have the potential to help increase this voltage.

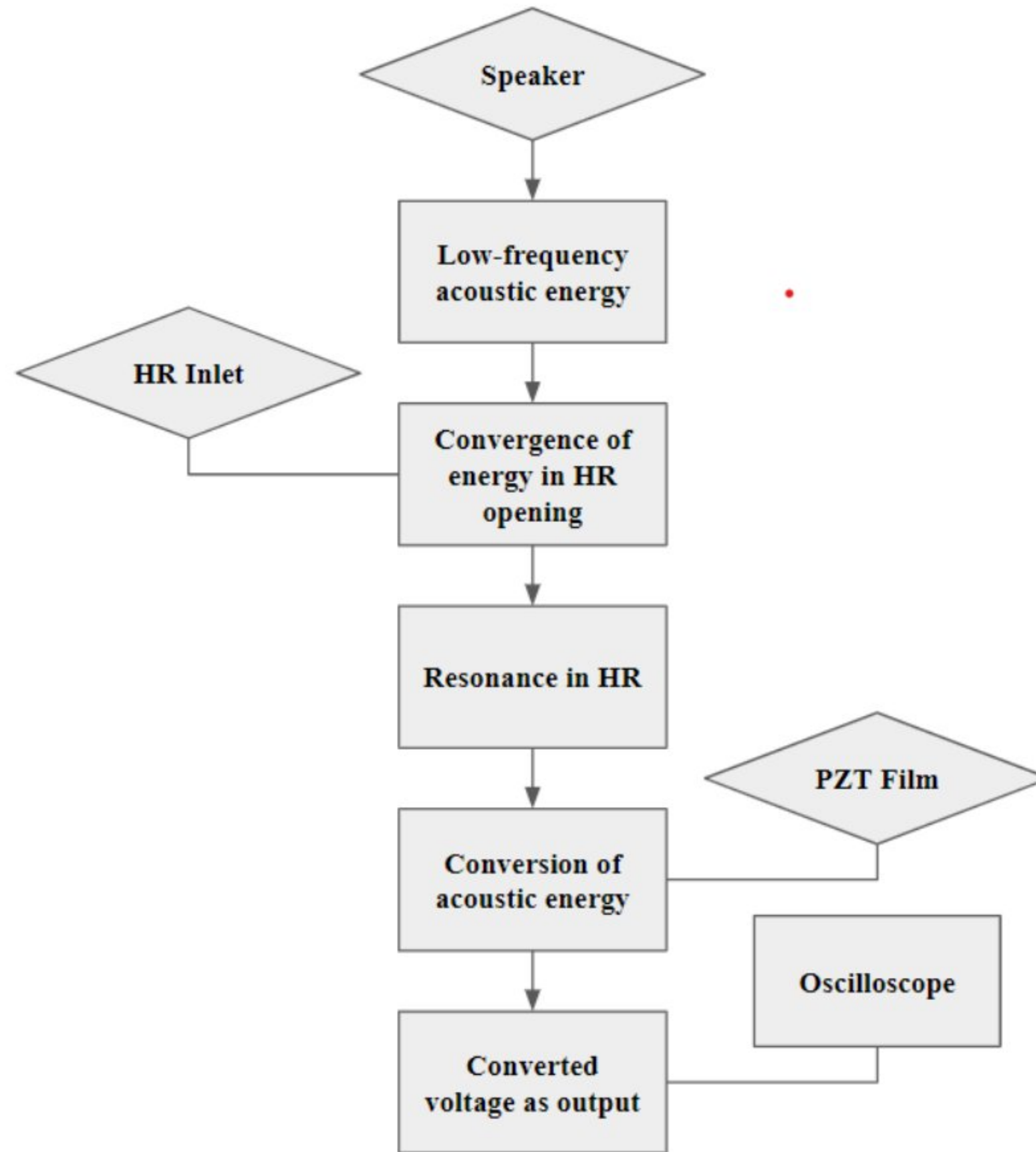


Figure 3.1: The architecture of the study.

3.2 Geometry

The primary geometry of this study is the size and shape of the resonator. While working with the resonator unit, the primary concern was to innovate a shape that could be easily multiplied into a noise barrier or an array to get a usable collective output. Hence after considering many other shapes, the resonator was designed, and the size and dimensions were picked by trial and error. There are two sections of geometry to analyze. One is for the unit-based output, and the other is for the implementation-based output. Both geometries are essential for this experimental work process, and they are described as follows:

1. **Single Unit of Helmholtz Resonator**
2. **Array Design of Helmholtz Resonator**

3.2.1 Single Unit of Helmholtz Resonator

To conduct the study smoothly and efficiently, a single resonator unit was first used. Since the array is a collective arrangement of multiple single units, it is sufficient to study the output of one unit and adjust the total production accordingly. While manufacturing the 3D model of the single-unit resonator, multiple factors were considered and acknowledged. The dimensions, characteristics, and even the materials were considered to come up with the best possible design, as shown in **Figure 3.2**. One of the biggest concerns was whether to change the shape of the unit or keep it the same as the previous hexagonal design. After an in-depth study, it was determined that the resonator setup should be kept in a hexagonal form, as optimizing most of the available space is a great concern for this research. As mentioned in the study by Anayet et al. [1], hexagonal shapes are the most optimized shape for utilizing space. Hence the resonator was kept in the same shape depicted in **Figure 3.2**.

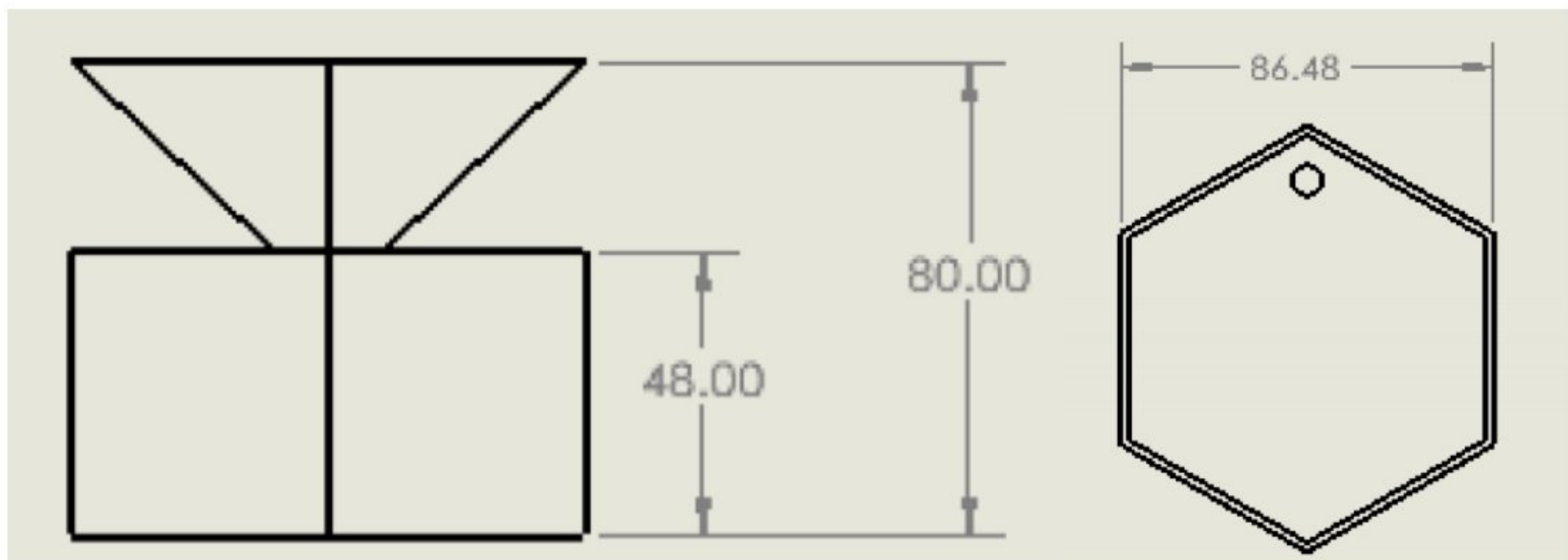


Figure 3.2: Front and Bottom view of the prototype along with dimensions. [1].

However, differing from the previous study, it was found that while keeping the resonator shape unchanged, the inlet designs could be optimized for better convergence of the inflowing vibration. In accordance with that, two alternative designs were suggested and then implemented, as discussed in the future works part of this study.

3.2.2 Array Design of Helmholtz Resonator

In addition to the single unit, a 3D design was also designed by Anayet et al. [1] in SolidWorks for the array configuration of the resonator. **Figure 3.3** [1] shows the array design configuration and how it can be accumulated by using multiple single units simultaneously. This array configuration can be simply obtained by enforcing multiple units of the same single-unit models discussed in the last paragraph. The array is a serial connection of multiple resonators to provide better output and an understanding of the noise barrier and how it will work. The noise barrier is one of the main points of future work, which will be discussed later in the result and discussion chapter. This array design is for installation at different establishments from where the noise will be harvested. This array will consume the vibration energy on a larger scale and provide better sound performance.

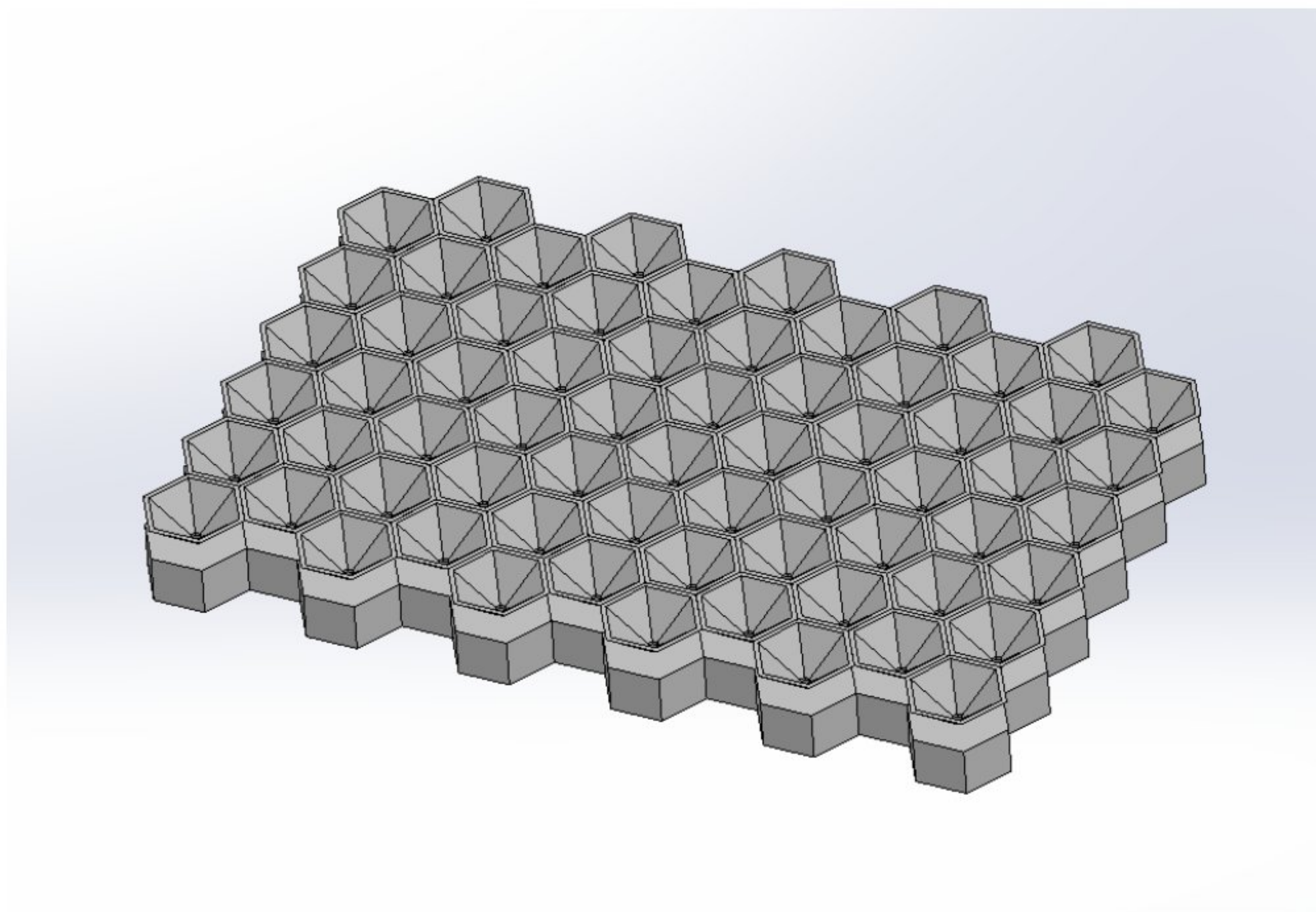


Figure 3.3: Array design of the prototype for the noise barrier. [1].

3.3 3D Printing Machine

To convert the CAD model into a physical model, the X30 model made by CCH Teknoloji was used, as shown in **Figure 3.4**. The printer, along with other variants of it, is present in the Cezerei Lab in IUT. The main CAD file is first converted into STL format to input to this 3D printer. Afterward, it was put into the printer through a pen drive. Polylactic acid (PLA) was the material for this prototype as it is a well-known and readily available material. Around 6-7 hours were needed to build the prototype. After that, the model was maintained for further work in our experimental process. The support structures were removed, and the entire printed structure was given a proper finish to produce a high-quality print.



Figure 3.4: 3D printing machine.

3.3.1 3D Model

The 3D model was generated from the designs with the help of the aforementioned 3D printer by more than 30 hours of work. While printing the model, multiple factors were kept in monitoring to maintain the quality of the printed unit. Ports were kept in the design to connect the PZT films with the setup. The prototype is demonstrated below in **Figure 3.5**, along with the detachable base plate setup.

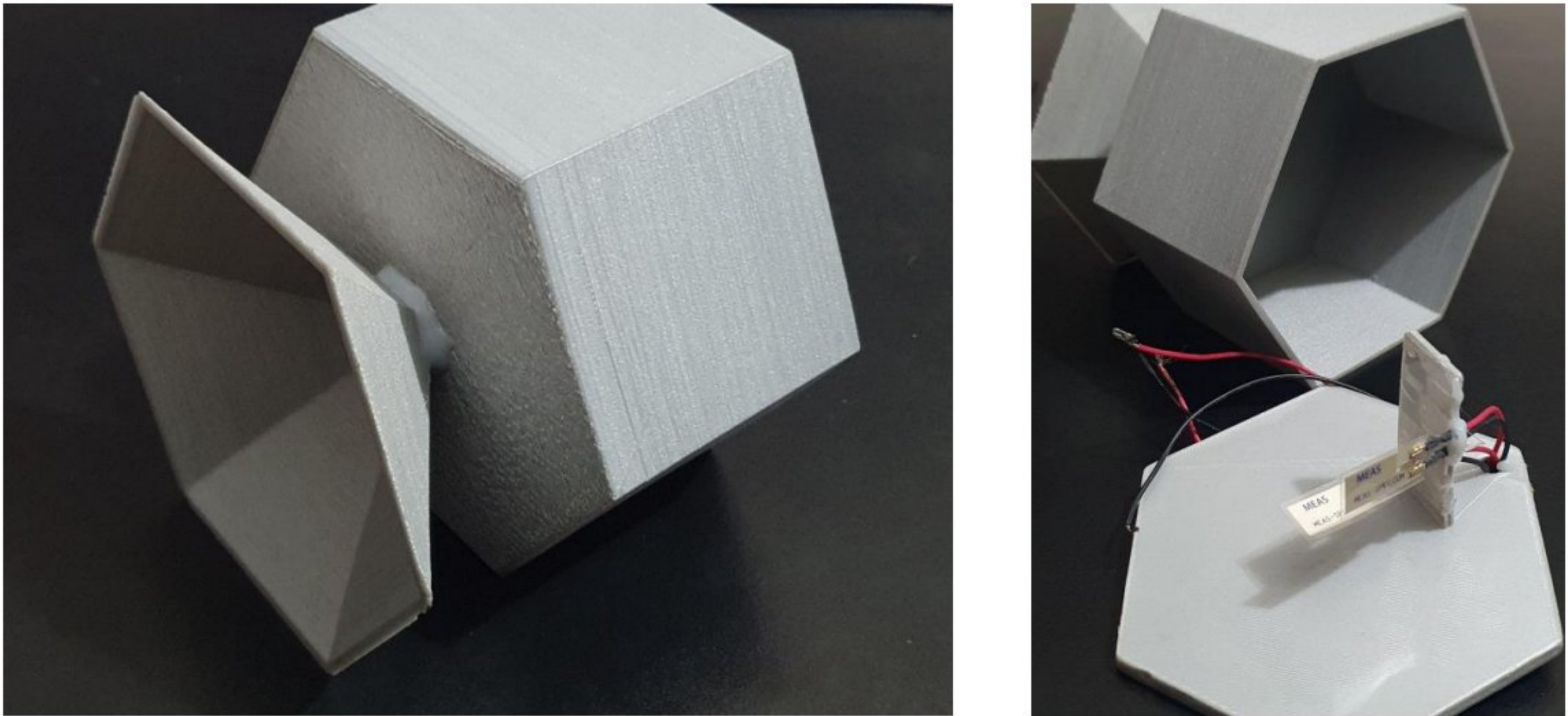


Figure 3.5: Assembled and disassembled views of the prototype.

The figure perfectly demonstrates the build and configuration of the prototype in assembled and disassembled state. The bottom part of the resonator is detachable, and the beam to connect the films is situated perpendicularly on the base plate. Necessary ports are made on the beam and also on the base to accommodate the wirings and enable the assembly of the films in different configurations. The base plate is easily detachable to help change the orientations or do necessary work. In addition to that, this allows the prototype to have better portability and overall accessibility. However, the base plate was printed with such care that when assembled, it helps the cavity to be completely disruption-free and increases the accuracy of the results.

3.3.2 Modified 3D Models

The output of the resonator greatly depends on optimizing the amount of vibration energy utilized by the Helmholtz resonator. The vibration energy enters the resonator through the neck area, creating excitement in the PZT films. The excitement then generates voltage and shows output reading on the multimeter. To do that more efficiently, converging the vibration energy onto the film surface is a crucial issue. The inlet part of the Helmholtz resonator does this converging action. If the design of the inlet can be optimized in a way that helps create a better-converging effect on the incoming vibrations, the outputs can significantly improve. To do this, innovative and more efficient designs of the inlet structures were included in this alternative approach. The considered structures are shown below in **Figure 3.6**.

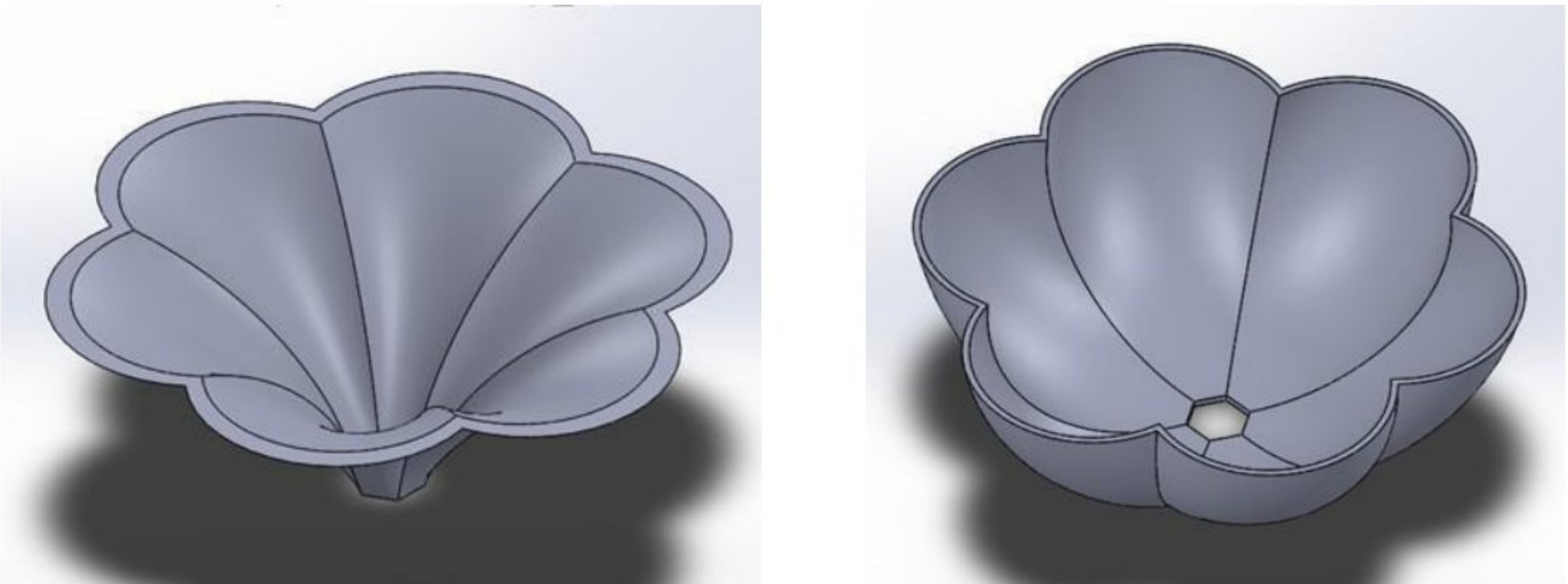


Figure 3.6: Converging and diverging designs for the new inlet.

Based on these designs, further experiments were conducted to see how the output results changed. These two designs depict the output change due to the bending of the converging surface. The converging and diverging designs allow the converging vibration to follow a contoured output before entering the resonator cavity through the neck area. Comparative studies were done on output voltages based on previous studies. Such inlet designs are expected to converge the incoming vibrations better and provide better results. Results from this alternative are discussed in the results section.

3.3.3 Orientation of the Films

The orientation of the PZT films inside the resonator has a tremendously important role to play in this study. The vibration energy entering the resonator is first converged by the inlet. Then it enters the resonator through the neck area. After entering, it creates excitement in the PZT films. It depends solely on the design, orientation, and placement of the films on how efficiently the prototype will work. Improving the film orientation, exposing the films to capture the excitement better, and systematically regulating the film behavior can prove to be vital aspects of this study.

In the previous study done by Anayet et al. [1], the double film configuration was implemented using a parallel orientation. The cantilever theory was used, and two films were set on top of one another at a distance. The films were horizontally parallel to each other while. **Figure 3.7** [1] demonstrates the previous setup perfectly. Among the two, one film was a bit extended, namely the lower film, and the other film was shortened. This was done to make sure both films got an ample amount of exposure to the resonating vibrations.

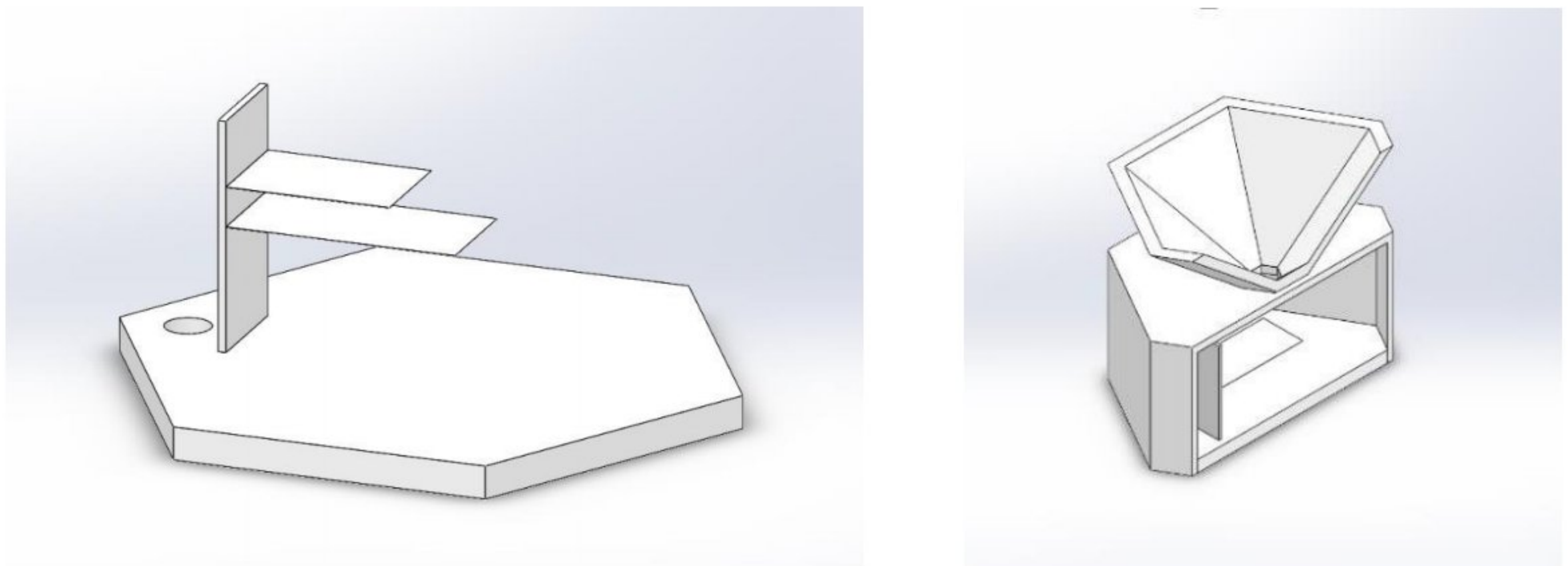


Figure 3.7: Film orientation of the previous study.[1]

This orientation was later changed to perpendicular orientation in this study to help understand the effects of orientation change potential of the new orientation and to generate better output which is depicted in **Figure 3.8** below.

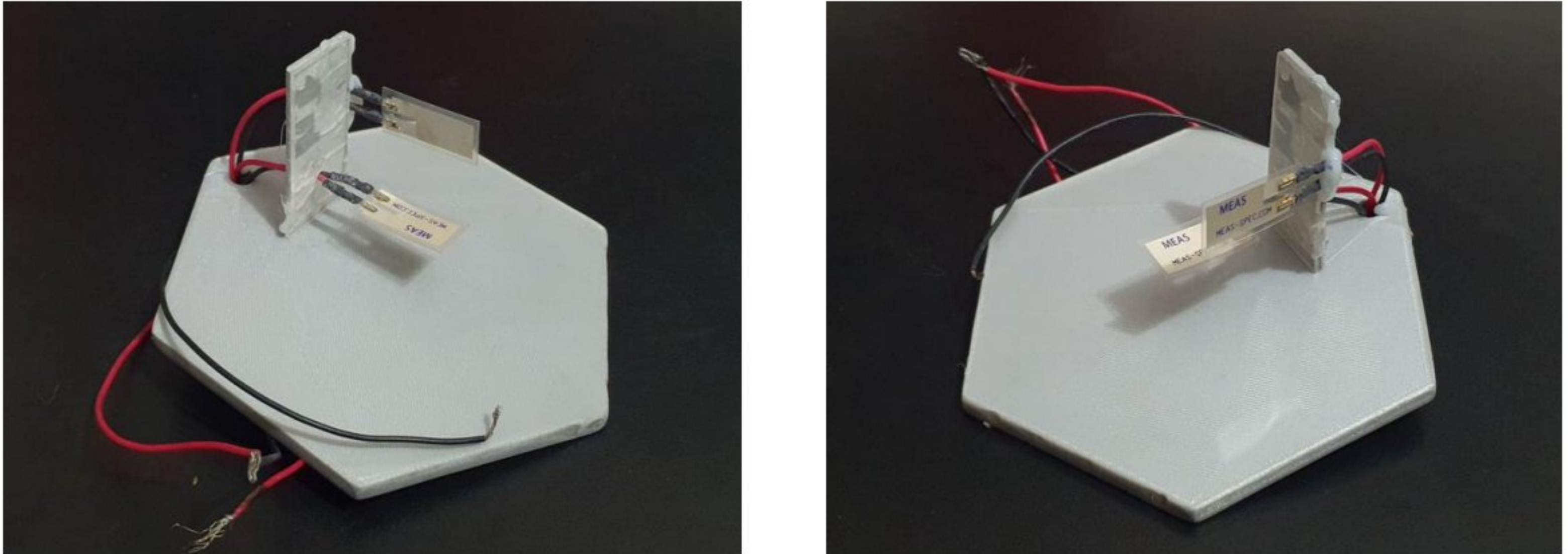


Figure 3.8: Film orientation of the new prototype.

The view in **Figure 3.8** perfectly demonstrates the orientation of the films in a perpendicular configuration. In this setup, both films are attached to the inner beam of the prototype through a glue gun. The attachment process must be done with extreme care to ensure that other impedance from surroundings can not affect the piezoelectric film. A handful of other factors are to be taken into account that could potentially disrupt the possibility of a good outcome, such as the sound from any surrounding sources and even unintended human pressure. Low-frequency vibrations enter through the prototype's inlet part, go through the neck, and the sound will create pressure in the piezoelectric film.

3.3.4 Orientation of Increased Films

To modify the setup and improve outputs, our following approach will be to increase the number of PZT films. Multiple PZT films have been proven to provide better output results in the previous study. Expanding the number of PZT films might significantly change the process.

The main/ concept of this study is to improve the overall output of the resonator device by using the vibration pressure created on the PZT films. The more efficiently we can utilize the vibration incoming through the inlet, the better it can be used to generate an output voltage. That leaves a possibility that if the number of films in the cavity can be increased and oriented more efficiently, e.g., in **Figure 3.9**, the output may increase.

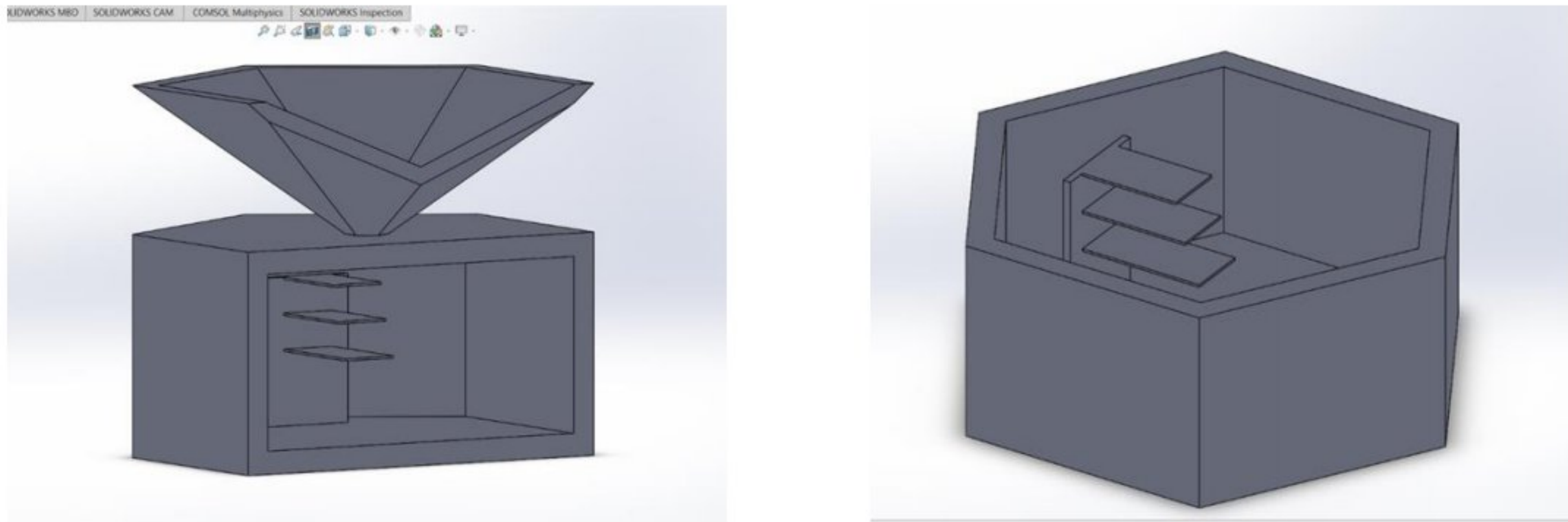


Figure 3.9: Triple film concept using the Helmholtz Resonator.

Some more designs of different film orientations will be formulated and then tested in the laboratory for possible outcomes under different conditions. However, it is to be kept in mind that changes in the number of PZT films might invoke irregular behavior in the output voltage. To help adjust and stabilize the outcome of the study, it may be required to find suitable adjustment criteria, such as different surroundings or temperature changes.

3.4 PZT Film Description

The most important part of this study is the Piezoelectric (PZT) films used in the experimental prototype. They are used to convert the exposed vibration energy into electrical energy. As the vibrational excitement reaches the PZT films, they provide the output voltage. How efficiently the prototype works or how well it will convert the vibration energy is solely based on the quality of the films. Although the orientation and configuration play an essential role in the process, it is important to use a good quality PZT film of the correct specification. This is mainly due to the possibility of disruption by the surrounding sources of noise. Good quality PZT films provide good results even when disruptive noise sources are present, which results in better output quality.



Figure 3.10: PZT film without resonating mass.

Specifications of the Piezoelectric films used in this study are stated in **Table 3.1** below:

Table 3.1

Specifications of the PZT films used in the experiment

Name:	Piezo Film Pressure / Vibration Sensor
Model No:	PVDF LDT0-028K
Output:	High voltage output
Package:	Thin film element, size: 13mm*25mm
Operating temperature:	0 ~ 70°C
Accuracy:	1.4V/g~16V/g
Power supply:	Passive
Features:	Broadband (0.001Hz~1000MHz), high sensitivity, high dielectric strength, low acoustic impedance, high stability
Type:	Piezo Film Cantilever
Typical applications:	Vibration detection, electronic targets, counter triggers, and vital signs monitoring.

Table 3.2

Properties of commonly used piezoelectric materials PZT–Lead zirconated titanate[40].

Property	Units	PZT
Relative dielectric constant	-	1000–4000
Piezo charge constant d31	pC/N	-600--100
Electro-mechanical coupling factor	%	30–75
Young's modulus	10^{10} N/m ²	6–9
Density	kg/m ³	7500–770

Different parameters of the piezoelectric film which was used for the experiment are shown in **Table 3.3**. The PZT film part generates more than ten millivolts per microwave, approximately 60 expanded its product than the voltage output of the slate strain gauge. Capacity is proportional to the area and roughly equal to the element's size.

Table 3.3

Different parameters of the piezoelectric film were used for the experiment. [1]

Part Number	1-1002149-0
Film Thickness	28 μm
Film	.64 (16)
Electrode	.484 (12)
Film	1.63 (41)
Electrode	1.19 (30)
Total Thickness (μm)	40
Cap (nF)	1.378

The PZT series testers are the simplest type of piezo film sensors, mainly used as flexible dial gauges and touch microphones for vibration or impact detection. These are usable without a lead for such systems that the user needs to make their lead connection. The sensors can be conveniently connected to the dual tape or epoxy board. Compressive clamping, crimping, eyelets, conductive epoxy, or low-temperature clamping can accomplish lead binding.

3.5 Sound Source

This study was done to demonstrate the idea of capturing low-frequency sound waves and generating voltages from the available vibration energy. It can be quite challenging to idealize such kind of noise or vibration for the environment or by natural means. Hence, a sound system of 2 speakers was used here to generate sound for testing. The input sound is measured in terms of the input frequency of the sound and is regulated very carefully. The sound was amplified by the power amplifier with an amplification factor of 1.1 and was gradually controlled by the function generator. The connection of the speakers to the system is explained in **Section 3.6** ahead.



Figure 3.11: Speakers (Havit HV-SK473) used in the experiment.

Below are the specifications of the speakers used in this experiment presented in **Table 3.4**:

Table 3.4

Signal / Noise Ratio:	84db
Frequency Response:	90 HZ-20KHz
Jack:	3.5mm
Impedance (Ohm):	4 Ohm
Output Power:	3W*2(RMS)
Power Input:	5v (USB)

3.6 Experimental Details

In this section, the part-by-part description is added for a clear understanding of the experimental setup. All the components and apparatus listed below are used for this study, and the connection of these components is an essential aspect of the research. It is to be kept in mind that the output of the study directly depends on the setup and its surroundings, as the results are easily disrupted by other noise sources.

Below are the components used for the experiment apart from the prototype:

1. Function generator
2. Oscilloscope
3. Power amplifier
4. Speaker

For the first part of the experimental study, the setup was kept unchanged for the most part. As per methodology, the existing results were first to be tested and verified. Then the orientation change mentioned in **Section 3.3.3** and as depicted in **Figure 3.8** was to be tested out. Hence the setup was re-constructed in the lab as instructed by the authors in the following setup of **Figure 3.12**.

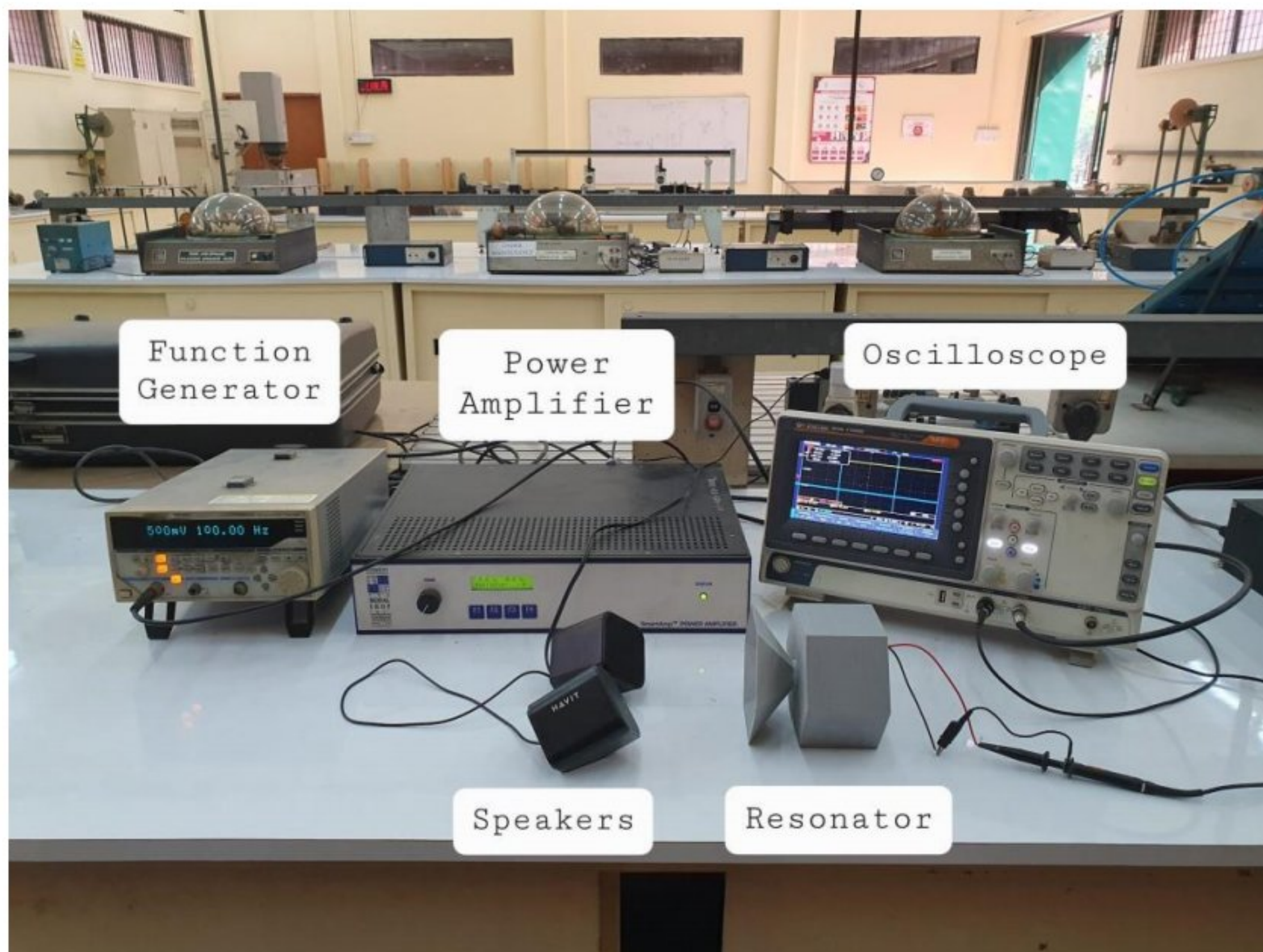


Figure 3.12: Physical demonstration of the experimental setup.

In the laboratory arrangement, all the components listed above were arranged accordingly. The function generator is to generate signals of desired characteristics and observes the PZT behavior. The output of the function generator was connected to the power amplifier input to amplify the signal to a desired level. The amplification factor was kept constant at 1.1 to get an expected sinusoidal wave output. The input of the speakers was connected to the power amplifier with the help of necessary wiring. This is done so that the sound output of the speakers can be easily regulated through the amplifier by changing the amplification factor. The oscilloscope was connected to the function generator output to help observe the wave characteristics of the generated signals while the experiment was going on. This also helped see the displacement of the PZT film under the provided vibration wave.

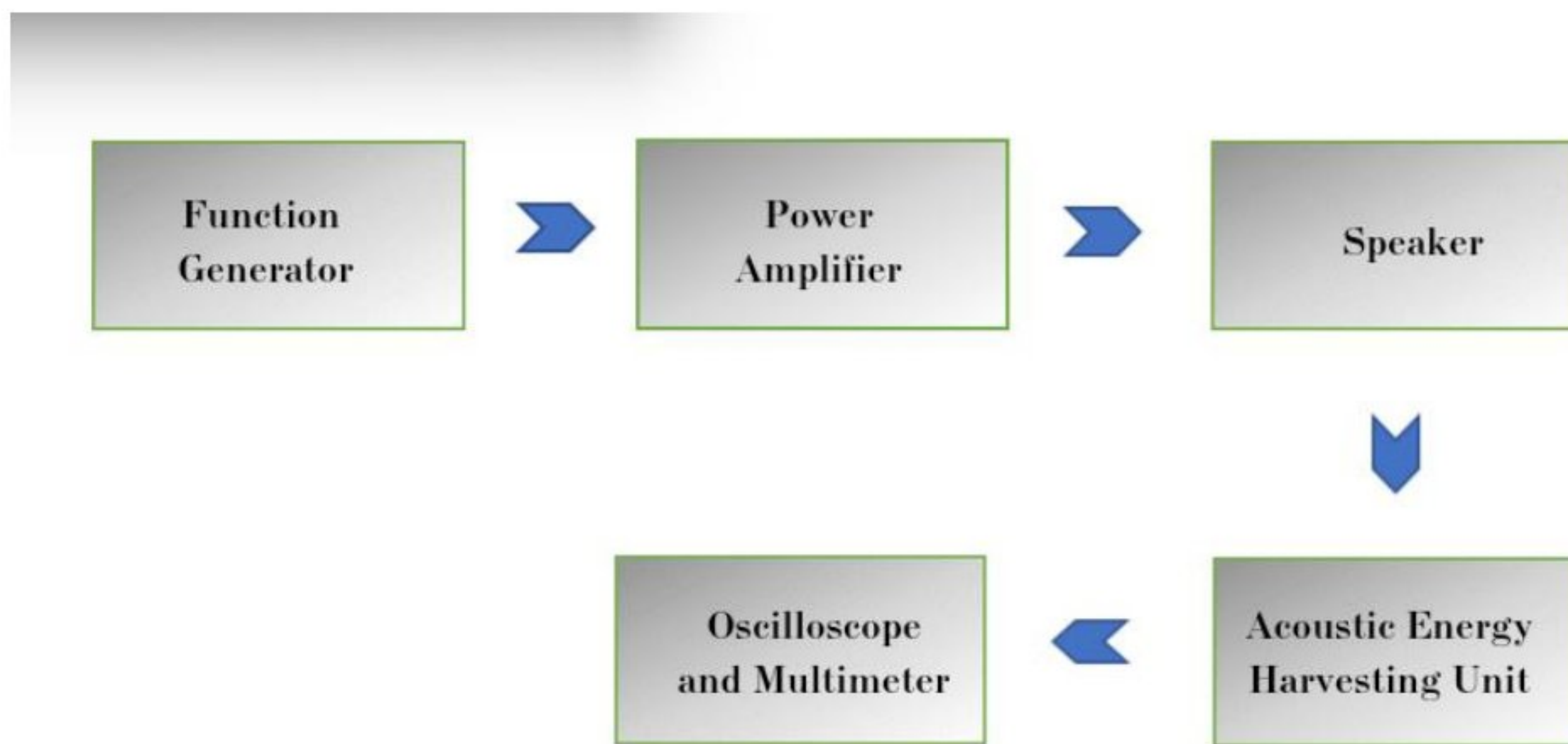


Figure 3.13: Flow diagram of the experimental setup.

The sound wave generated from the speaker will be amplified by a factor of 1.1 by the amplifier. This sound wave will go through the resonator inlet. The inlet will converge the waves, and this converged vibration will go through the neck part of the HR and enter the cavity. Inside the cavity, there will be displacement in the PZT films due to the impedance of the speaker. This will generate excitement in the PZT films, and voltage will be generated, which can be measured by a multimeter and stored data accordingly. The flow diagram of the experimental setup is shown in **Figure 3.13**.

3.7 Boundary Conditions

Boundary conditions are a set of assumptions and acknowledgments done to conduct experiments and observe the outputs with a clear perspective. During the performance of this study, a few boundary conditions were set for the interpretation of the results properly. These boundary conditions were set based on some primary assumptions and research philosophies in mind. The primary objective here was to observe and analyze the output with respect to the function generator input. Hence, the inputs and outputs were varied in the following way in **Table 3.5**.

Table 3.5

The input voltage and input frequency were varied, and the output voltage was observed.

Voltage	Frequency
500mV(fixed)	100Hz-200Hz(variable)
1000mV(fixed)	100Hz-200Hz(variable)

In addition to this, the amplification factor of the power amplifier was kept to 1.1. The distance between the speakers and the prototype was set to 100mm. This was determined based on the approximate distance where the two generated waves could intercept each other. Ensuring this is crucial for the study, so the equation of two individual waves intersecting each other was used.

- $Y=Y_1+Y_2$

Here, Y_1 and Y_2 are the wavelengths of the waves to be superpositioned, and Y is the superpositioned wavelength. Other conditions like temperature and air pressure were kept natural.

Chapter Four

Results and Discussions

4.1 Experimental Results

The acoustic vibration generated from the speakers converges on the resonator inlet and then enters the resonator. The vibration energy resonates with the walls of the HR and then creates excitement in the PZT films. PZT films generate voltage while there is excitement in the surroundings. The oscilloscope and multimeter record the voltage output from the piezoelectric film terminals to investigate the energy from the harvesting device. The results found by this study are represented through graphs and discussed briefly in the later section.

4.1.1 Single Film vs. Perpendicular Double Films

Figure 4.1 shows a comparison of graphs of two sets of readings. They are single films and perpendicular films. The input voltage was kept fixed at 500 mV.

Both graphs follow a similar type of path, and their values also come very close to each other. Because of the perpendicular arrangement, one of the two films got shallow exposure to sound waves. As a result, the output readings here came close to the single film arrangement.

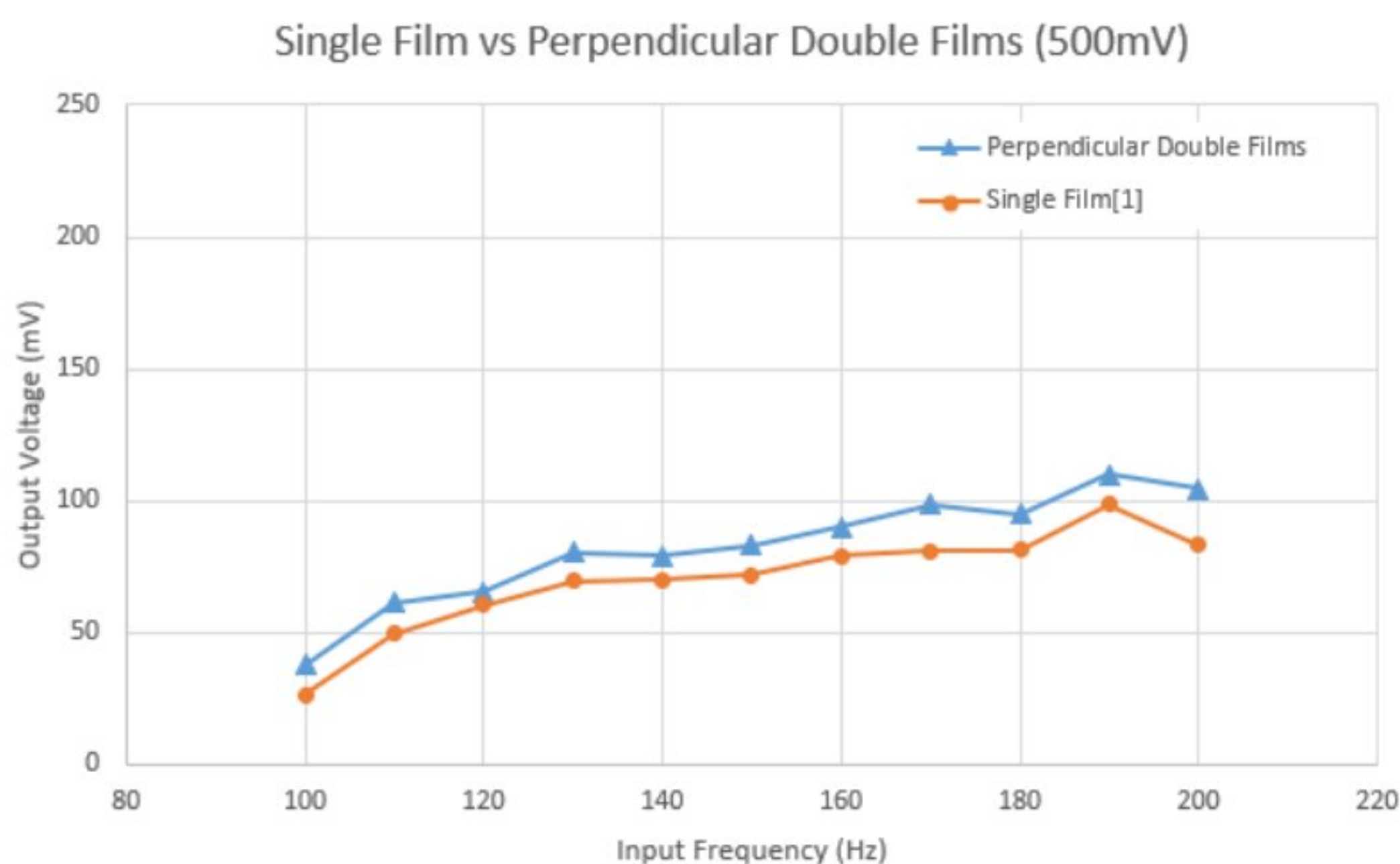


Figure 4.1: Output Voltage vs. Input Frequency at 500mV fixed input voltage.

The lowest value is found for the input voltage of 100 Hz. While a single film shows an output voltage of 26.487 mV, the perpendicular double films give an output of 37.868 mV. The same trend is seen for the peak values. For both configurations, peak values are found for 190 Hz input voltage, which is 98.513 mV and 109.89 6mV, respectively. This shows about 11% growth in output.

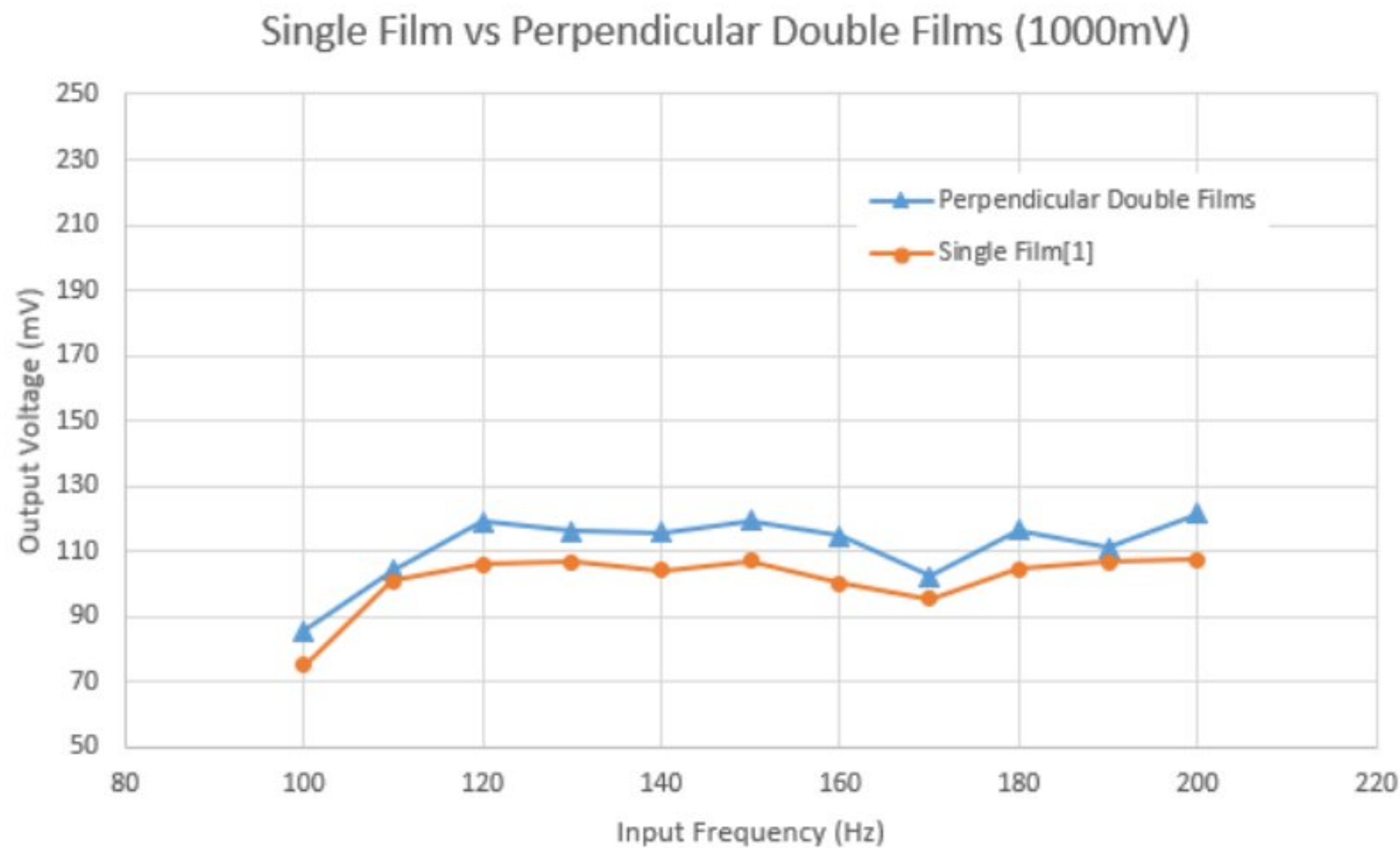


Figure 4.2: Output Voltage vs. Input Frequency at 1000mV fixed input voltage.

As we can see in **Figure 4.2**, The same experiment was done for a fixed voltage of 1000 mV. Results are seen to be quite similar to the previous case. Here the lowest voltage is generated for 100 Hz input frequency, 85.685 mV. However, peak voltage here can be obtained for a slightly higher frequency of 200Hz. The peak output voltage is 121.628 mV. Here, the gain is only 13% compared to the previous setup. The reason for the similar but higher output is that the double film setup has twice the number of films and can catch more distortion. However, due to improper exposure to the vibration, voltage is not generated as expected.

4.1.2 Parallel Double Films vs. Perpendicular Double Films

Figure 4.3 shows the amalgamation of two setups. Firstly, two films are arranged one below another in a parallel setup. Secondly, the two films are positioned perpendicular to each other. In both cases, the output of the setup while the input voltage was kept fixed at 500 mV.

For perpendicular arrangement, the highest output was 109.89 mV which was gained at the input voltage of 190 Hz. The second highest output was at 200 Hz, which was 104.653 mV. The previous inputs didn't bring better outputs. For parallel double film arrangement, the highest output comes at 170 Hz, which is 237.9 mV. The second highest output comes at 190 Hz, which is 230.9 mV. For both arrangements, the graph follows similar patterns.

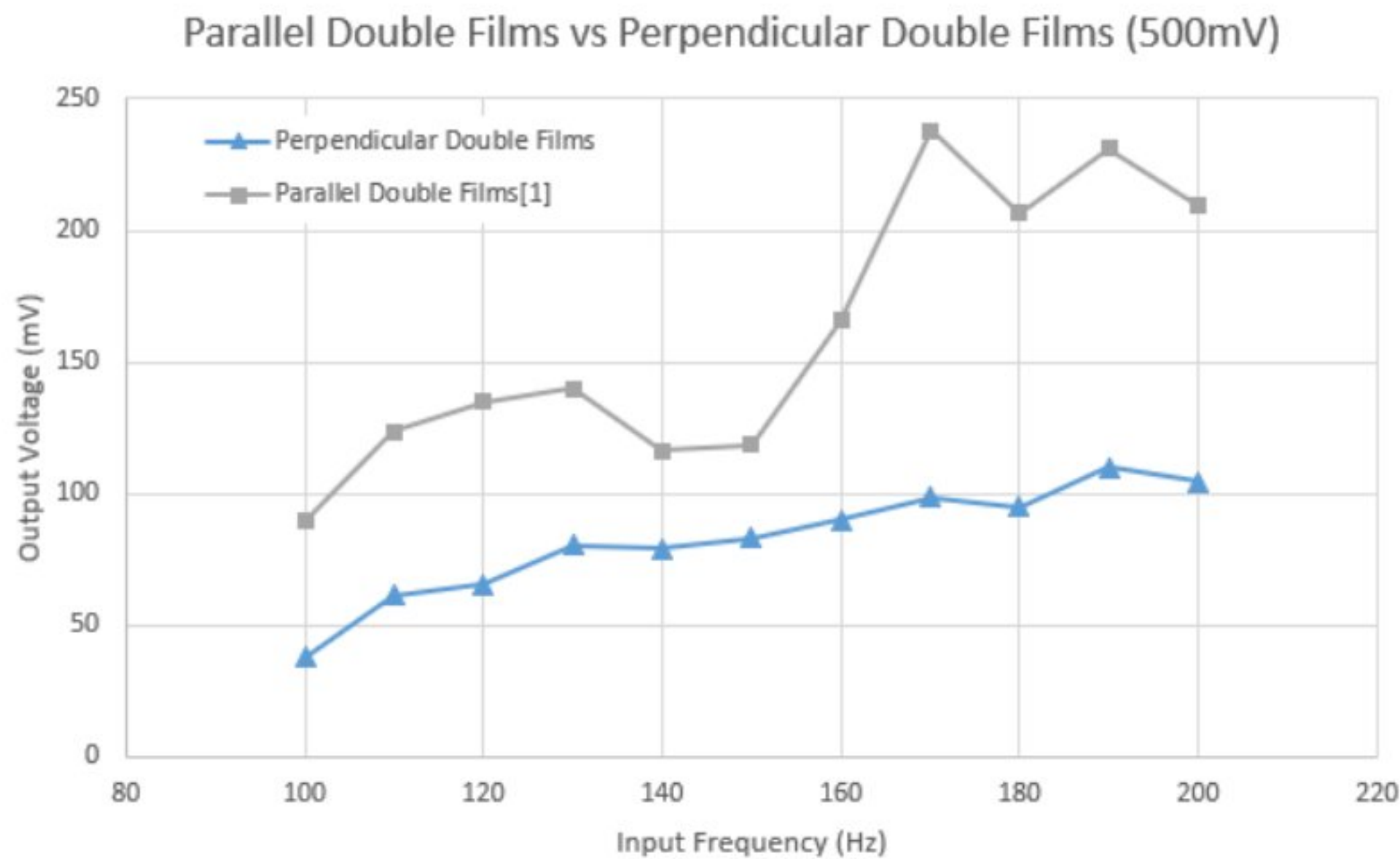


Figure 4.3: Output Voltage vs. Input Frequency at 500mV fixed input voltage.

Figure 4.4 represents the output of the same setup while the input voltage was kept fixed at 1000 mV. For perpendicular arrangement, the highest output was 121.62 mV which was gained at the input voltage of 200 Hz. The second highest output was at 150Hz, which was 119.42 mV. For parallel/double film arrangement, the highest output comes at 200Hz, which is 243.6 mV. The second highest output comes at 190 Hz, which is 231.2 mV. For both arrangements, the graph follows similar patterns. Although the results were very consistent throughout the frequency range, the outputs were not better than the previous output. This is due to the better exposure of the films in a parallel setup.

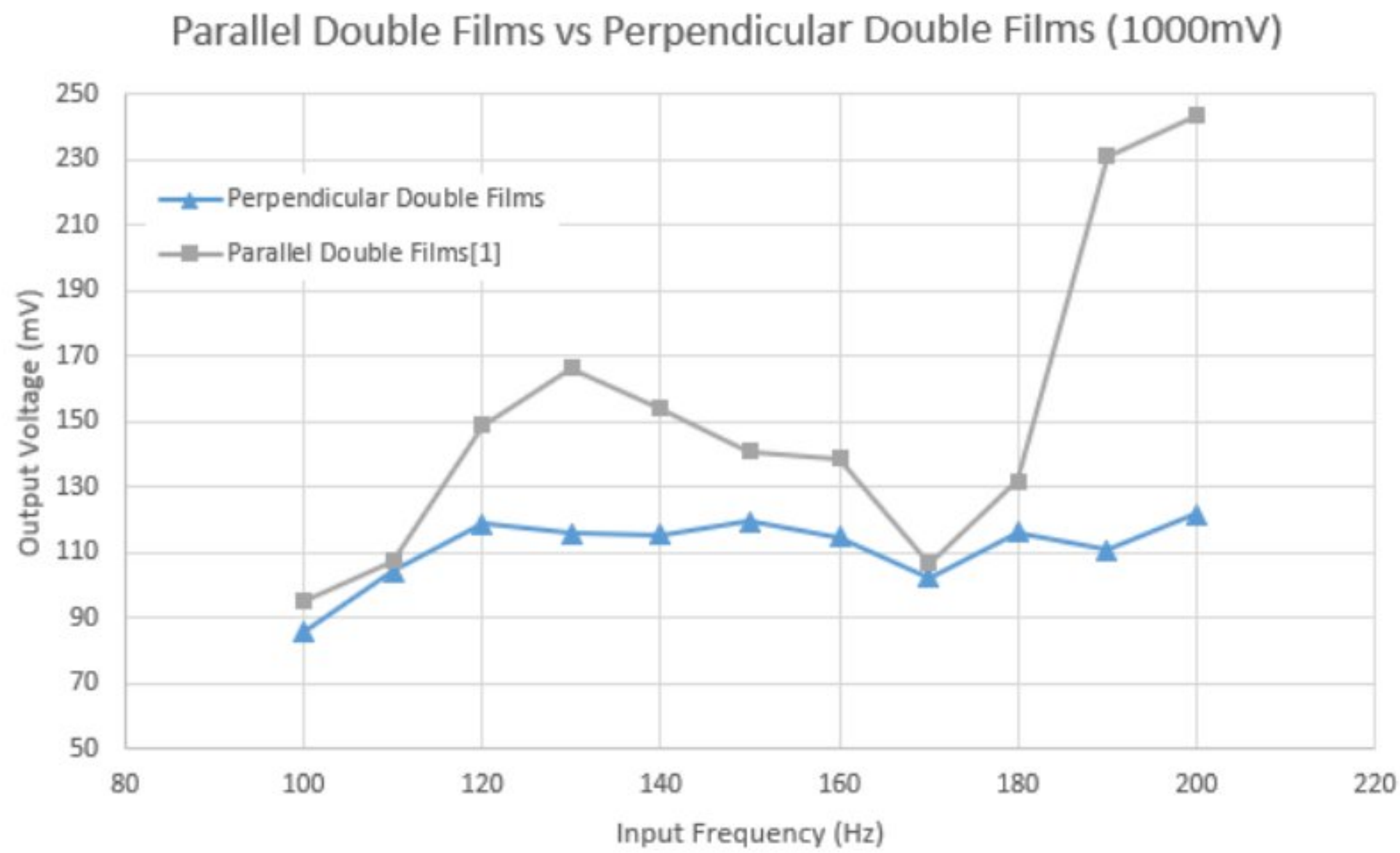


Figure 4.4: Output Voltage vs. Input Frequency at 1000mV fixed input voltage.

The outcomes primarily found in this study may show some fluctuations and irregular behavior due to disruptive noises from the surroundings. These noises, however, could be rectified with the help of soundproofing and background noise suppression. But, background noise suppression was not an option due to the experimental space's lack of soundproofing. The experimental setup was placed close to the speakers to reduce noise and inaccuracy.

4.2 Comparative Results

As this study was comparative research with the work done by Md. Anayet et al.[1], the results are analyzed in terms of deviation from that work. For each tested boundary condition, the output voltages are compared with the corresponding output voltages of the prior study, and discussions are made based on that. As depicted in **Figure 3.6**, output results were recorded for the configuration of the double film being placed perpendicular to each other inside the resonator. This orientation was done without changing the number of PZT films inside the resonator. Moreover, the inlet design was also kept the same for this configuration.

4.2.1 Single and Double Films vs. Perpendicular Films

At first, the data were collected while keeping the input voltage fixed at 500 mV and input frequency ranging from 100-200 Hz. The highest output voltage of the acoustic energy harvester is found to be 109.896 mV at 190 Hz frequency, as per **Figure 4.5**. Compared to the work before, this output has been found at a higher frequency. The previous study provided an output of 237.6 mV at a higher input frequency of 170 Hz.

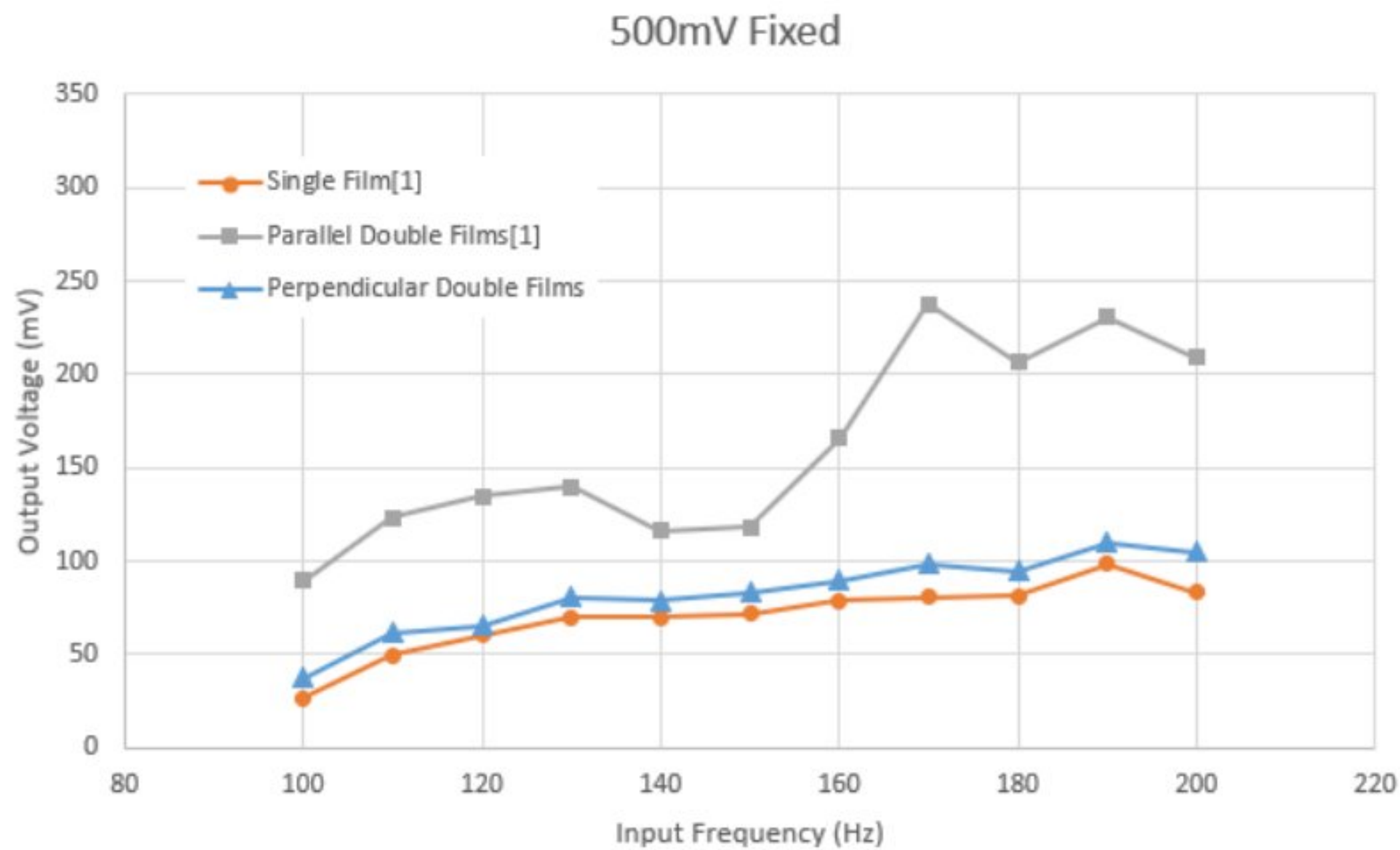


Figure 4.5: Comparison of output at 500mV fixed input voltage.

The same study was done while keeping the input voltage fixed at 1000 mV and input frequency ranging from 100-200Hz. As shown in **Figure 4.6**, the highest output voltage of the acoustic energy harvester is found to be 121.628 mV. This output is achieved while the input voltage is kept fixed at 1000mV and frequency at 200Hz. To compare with the previous work, the highest output here is obtained for the exact same frequency of 200Hz. But the gross output voltage of 243.609 mV is much higher than the current output of 121.628 mV. In two different ranges of input voltage, the previous setup gives almost twice the output of the new setup. This assures that the previous setup in parallel orientation was significantly better than the current one, even at higher input voltages like 1000mV.

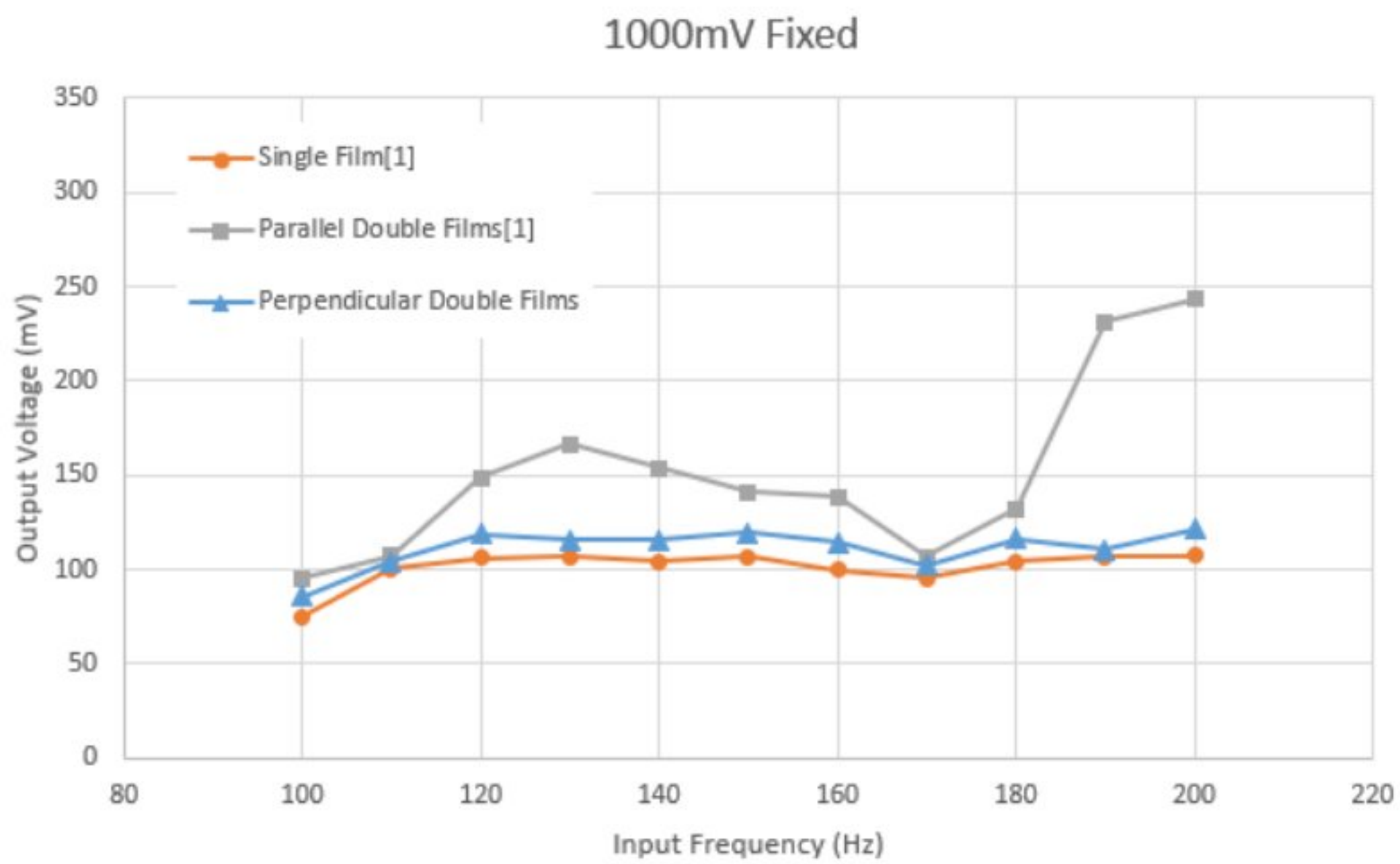


Figure 4.6: Comparison of output at 1000mV fixed input voltage.

4.2.2 Single and Double Films vs. Triple Films

After conducting experimental analysis on perpendicular double-film setups, it was found that the parallel double-film setups provide better results. Hence in the persuasion of better output voltages, the number of films was increased, and three films were used in a parallel orientation where the following results have been obtained.

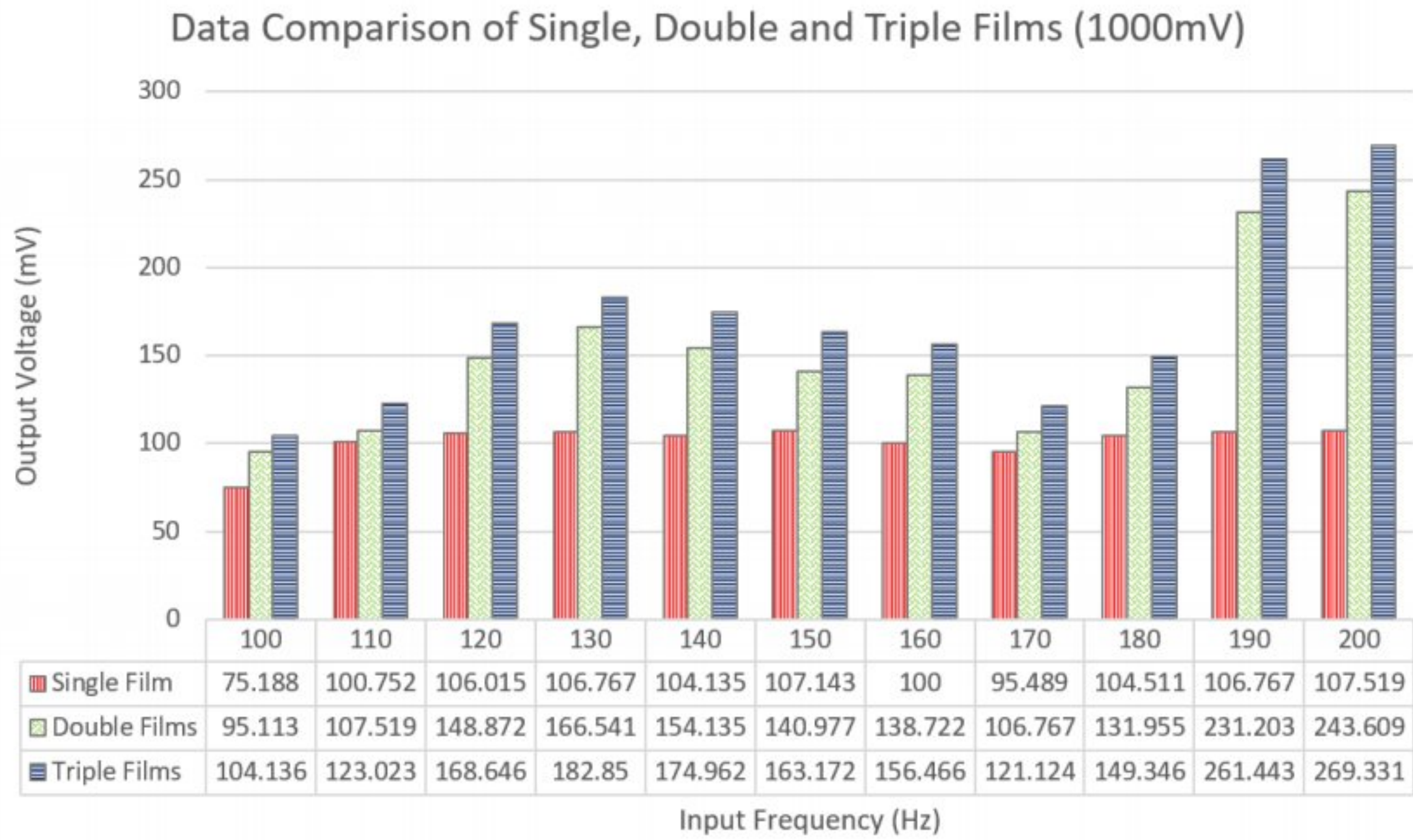


Figure 4.7: Data comparison for triple films at 1000mV fixed input voltage.

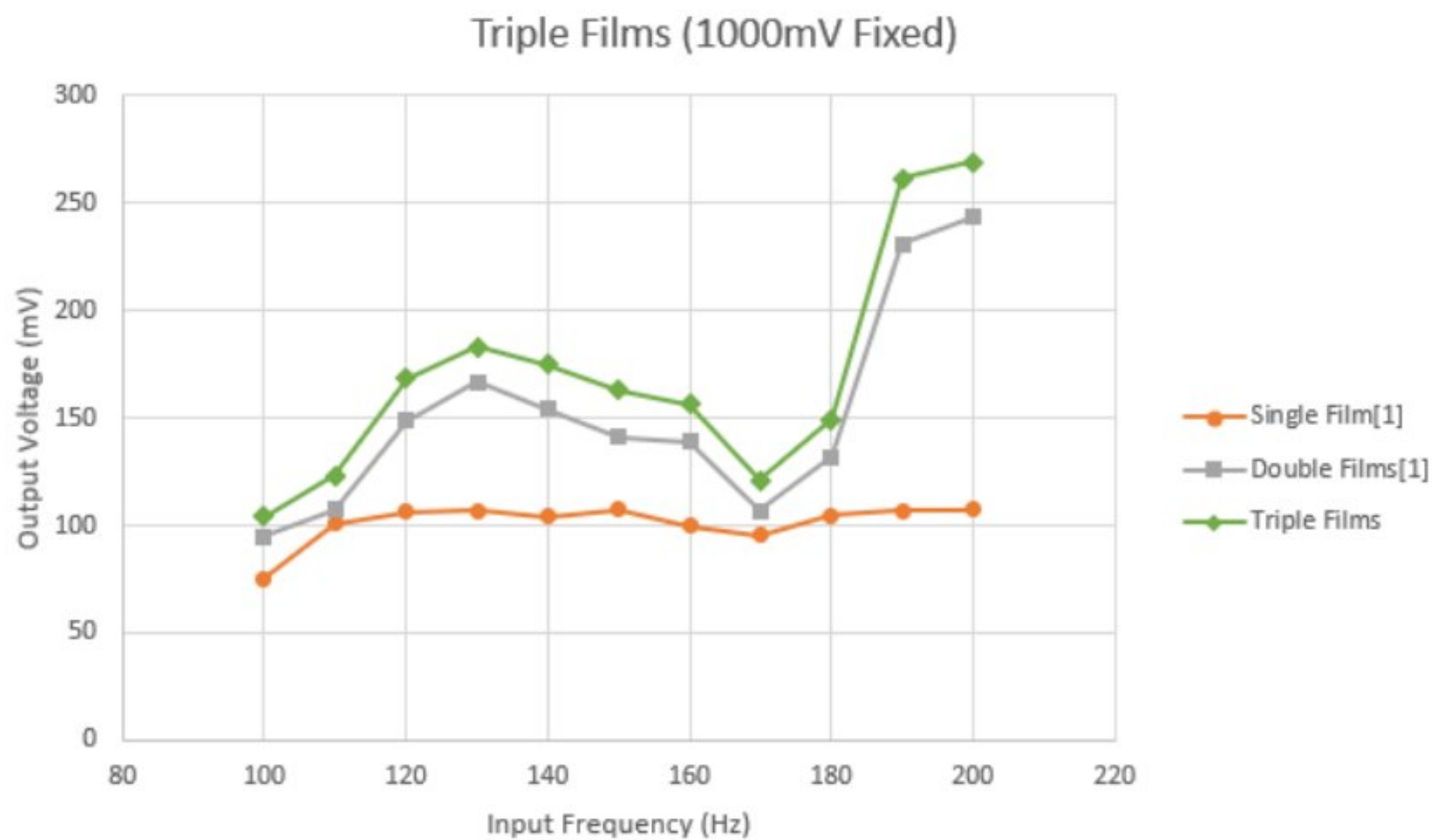


Figure 4.8: Comparison of output for triple films at 1000mV fixed input voltage.

The data were initially gathered using an input frequency range of 100-200 Hz and a fixed input voltage of 1000 mV. According to **Figure 4.7** & **Figure 4.8**, the acoustic energy harvester's maximum output voltage is discovered to be 269.3 mV at a 1000 mV fixed input voltage in the case of three film configurations. This output is observed when the input frequency is 200 Hz. This output has been observed at a significantly higher value than in the earlier work. The output of the earlier investigation was 243.6 mV at an input frequency of 200 Hz, which was in the case of double film.

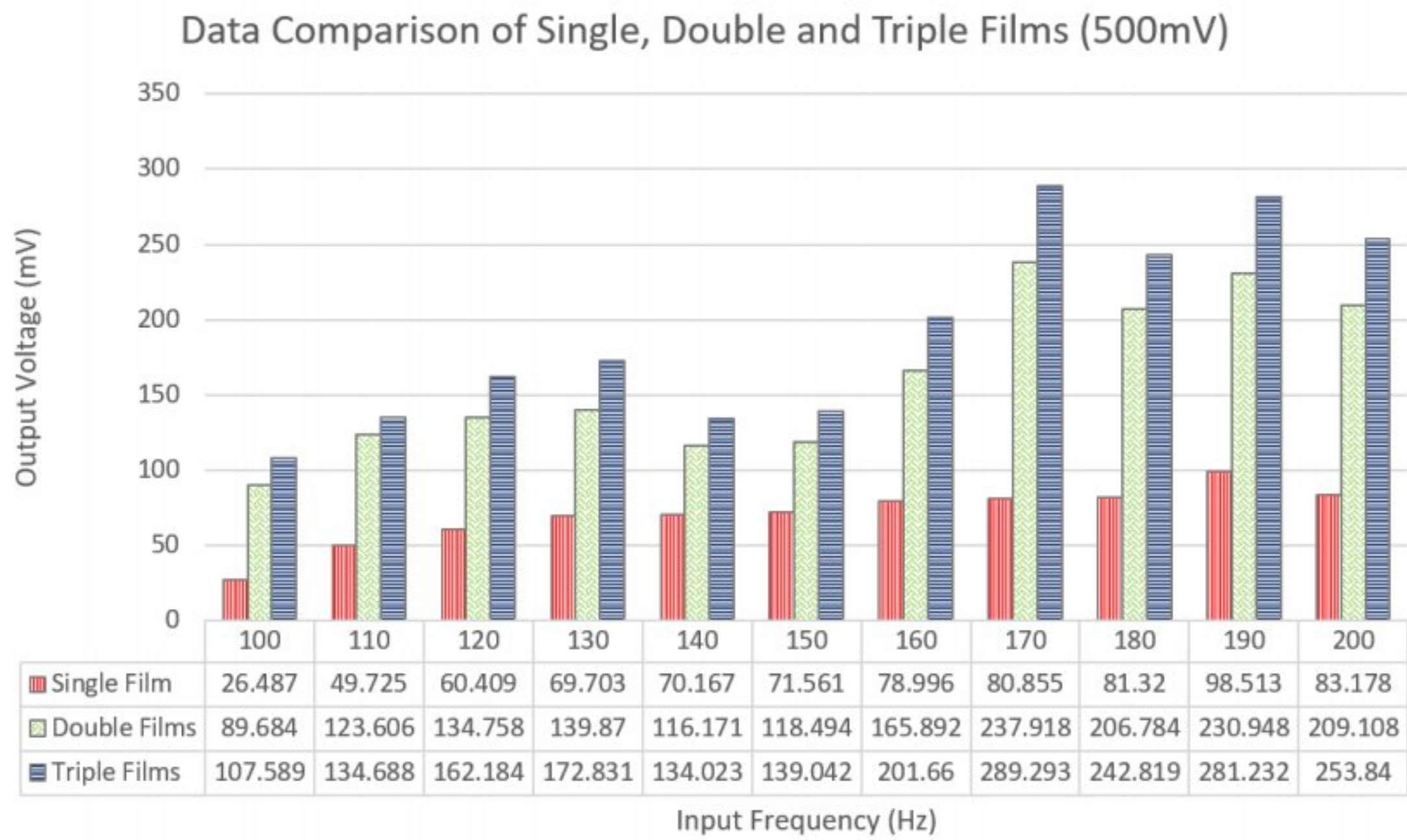


Figure 4.9: Data comparison for triple films at 500mV fixed input voltage.

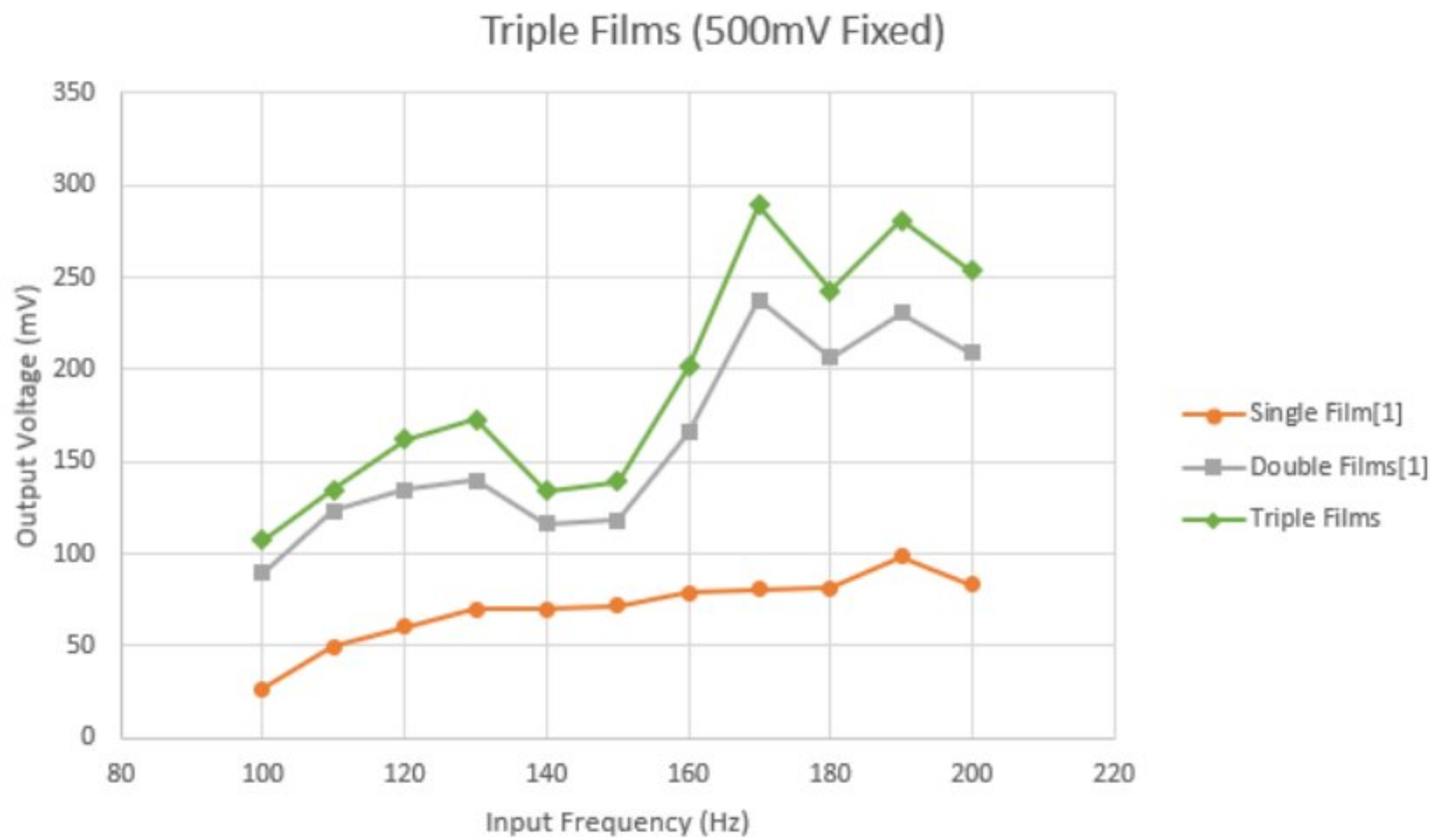


Figure 4.10: Comparison of output for triple films at 500mV fixed input voltage.

The same study was carried out using an input frequency range of 100-200 Hz and a fixed input voltage of 500 mV. The acoustic energy harvester's maximum output voltage is discovered to be 289.2 mV, as illustrated in **Figure 4.9** & **Figure 4.10**. This output is produced when the input voltage and frequency are fixed at 500 mV and 170 Hz, respectively. The highest output in this work is produced for a frequency that is identical to their earlier work. The current output voltage of 289.2 mV is a much better result than the total output voltage of 237.9 mV. So, we can see that both in the case of fixed 500 mV and 1000 mV input voltage, three film configuration gives better performance than the double film configuration.

4.2.3 Triple Films in Original vs. Converging vs. Diverging Inlets

The results were first acquired using a fixed input voltage of 500 mV and an input frequency in the range of 100-200 Hz. In the case of a converging inlet, **Figure 4.11** & **Figure 4.12** shows that the acoustic energy harvester's highest peak voltage is 272.9 mV at a 500 mV set input voltage at an input frequency of 170 Hz. Meanwhile, in the case of diverging inlet, the highest peak voltage is 271 mV at 190 Hz input frequency. The overall values of the converging inlet are slightly better than that of diverging inlet though their pattern in the graph is quite similar. When compared to the preceding work of the original shape inlet, this production has been seen at a substantially greater value. The output of the preceding research was 289.2 mV at an input frequency of 170 Hz.

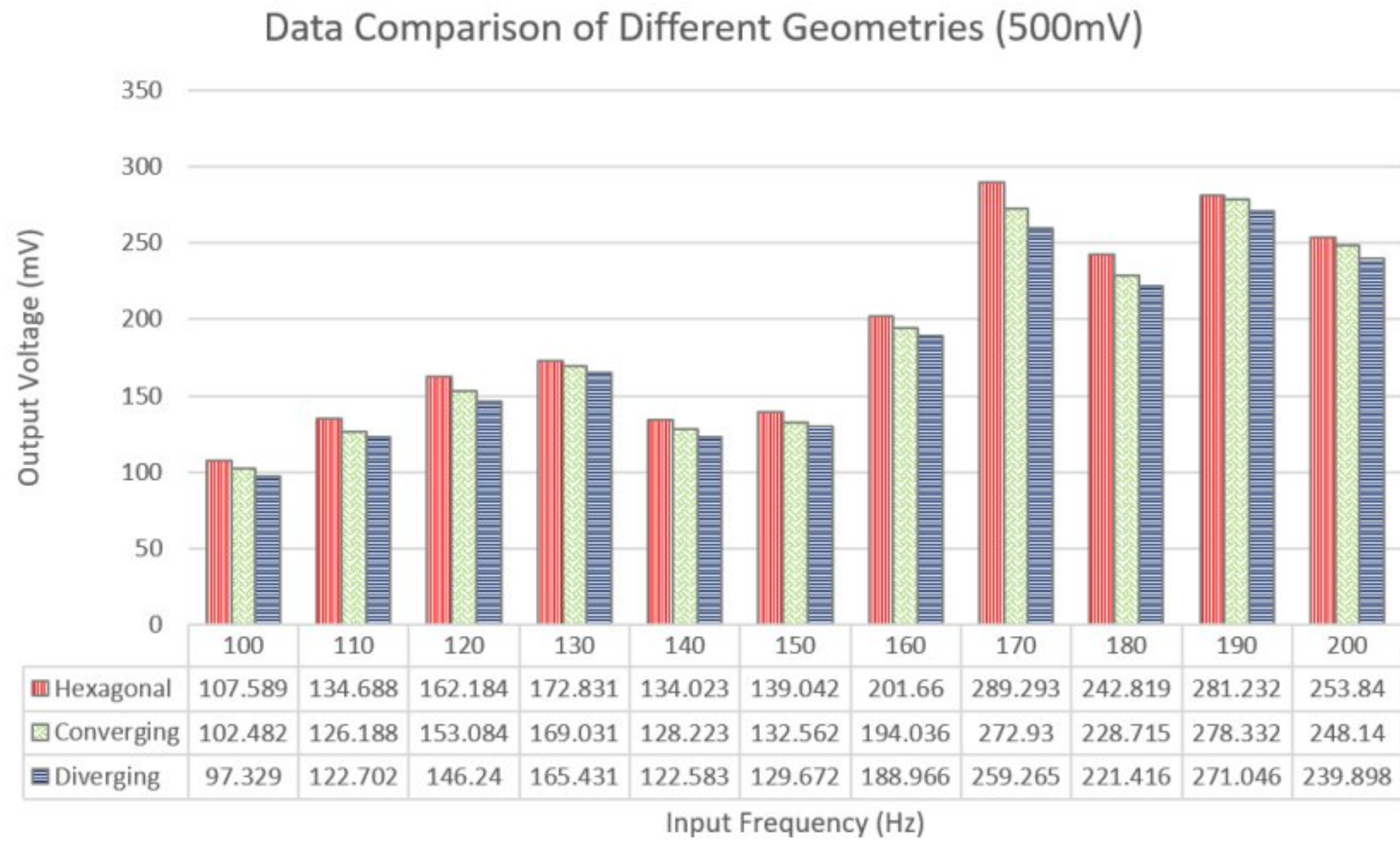


Figure 4.11: Data comparison for triple films at 500mV fixed input voltage.

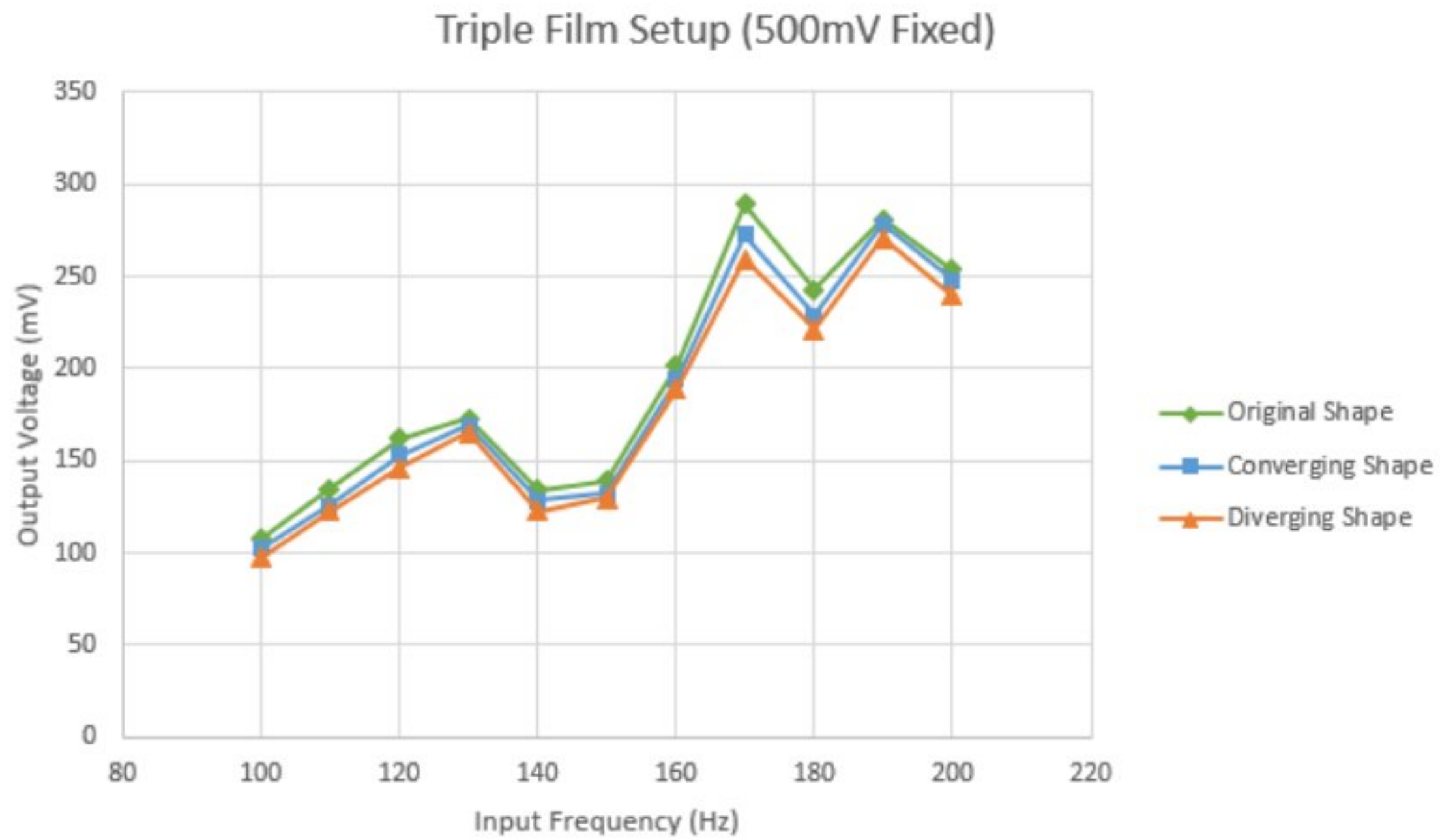


Figure 4.12. Comparison of output for different inlet designs at 500mV fixed input voltage.

The same study was done in the case of 1000 mV fixed input voltage at the range of 100-200 Hz. Frequency **Figure 4.13 & Figure 4.14** illustrates the sound harvester's greatest peak voltage of 256.6 mV in the converging inlet scenario with a 1000 mV set input voltage and 200 Hz input frequency. The maximum peak voltage in a diverging inlet scenario is 248.7 mV at 200 Hz input frequency.

Figure 4.13: Data comparison for triple films at 1000mV fixed input voltage.

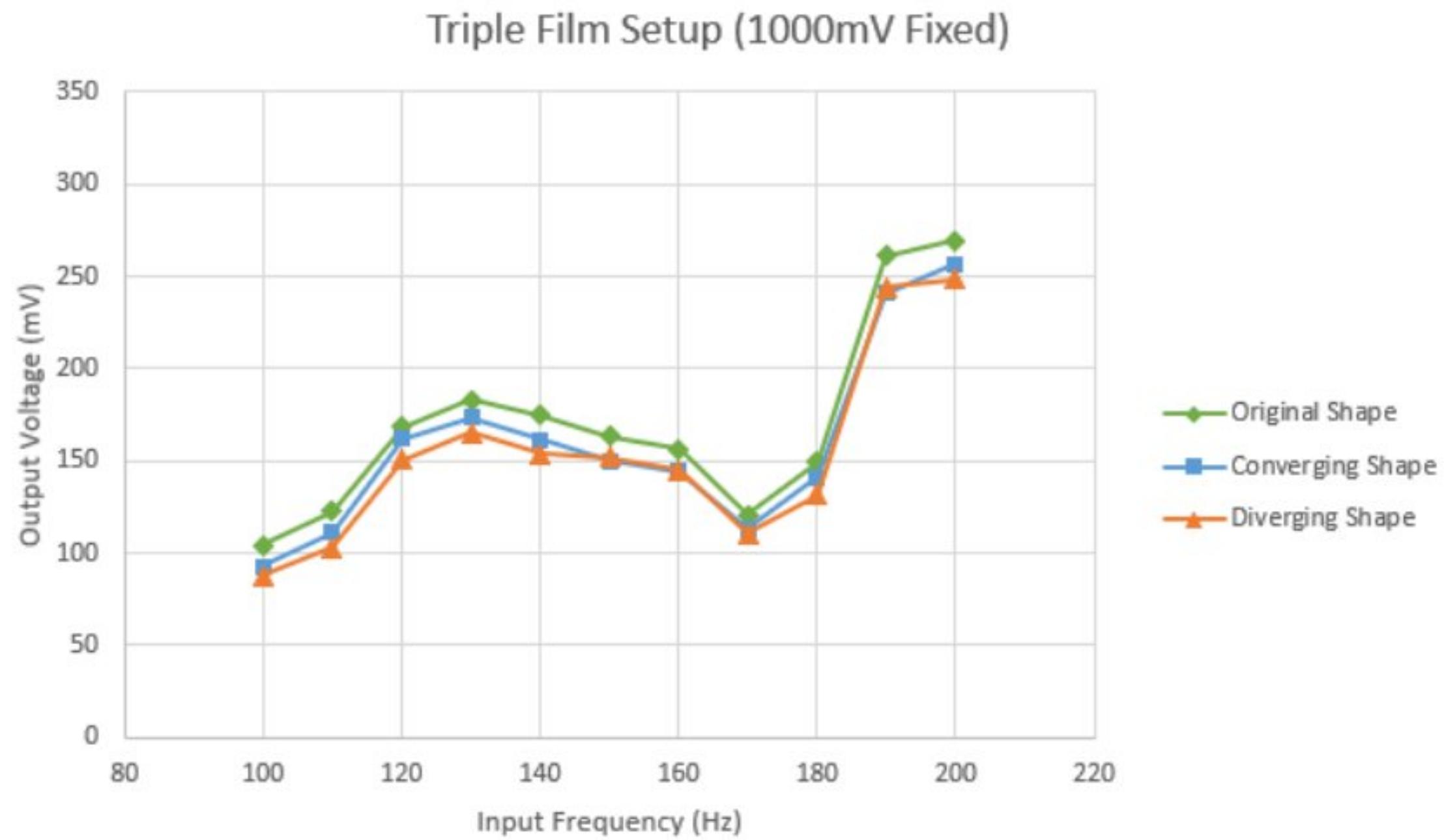


Figure 4.14: Comparison of output for different inlet designs at 1000mV fixed input voltage.

Despite having a very similar graph pattern, the converging inlet has somewhat better overall values than the diverging inlet. This output has a significantly higher value as compared to the earlier work of the original form inlet. The result of the earlier study was 269.3 mV at a 200 Hz input frequency.

Chapter Five

Conclusion and Future Scopes

5.1 Summary

After carefully considering the results of this experiment, the following things can be summarized:

1. The prior study of parallel film orientation provides a much better output voltage for the same input parameters.
2. Although the perpendicular setup provides a better output than a single film, it is significantly lower than the parallel orientation.
3. The reason for a lower output by the new setup is that the perpendicular film does not get much exposure to the vibrations as the deflections are not adequately conveyed.
4. The use of a second film narrowly provides a better result than the single film setup for the scattered vibrations caught by the second film.
5. The honeycomb structure may be further enhanced by experimenting with other intake shapes with a finer neck finish.
6. The experiment should be conducted in a noise-free lab where background noise may be canceled, negating the possibility of outside noise interference.
7. The Helmholtz resonator structure can be geometrically analyzed and utilized to better respond to the PZT film.

5.2 Future Scopes

While this study aimed to achieve an optimum solution for developing a prototype to harvest low-frequency acoustic vibrations with an affordable cost standard, the authors imply that there are huge scopes for development in this sector. As depicted throughout the study that there are different aspects of the experimental setup that can be focused on to improve better, more efficient results.

The number of PZT films, the orientation of the PZT films, and improving the resonator designs or inlets are a few factors that the authors considered and modified to the best of available knowledge and timeframe. More research can be done, and efficiency can be potentially improved by implying more innovative modifications to these aspects.

Besides the explored alternatives, future experiments may produce better results using a Helmholtz structure on a PZT material with improved acoustic impedance. The location and development of the film structure in the resonator can be worked on in the future. Including a diaphragm and more carefully regulated sound energy input can produce better outcomes and aid in obtaining more precise results.

5.3 Conclusion

In this experimental study, a low-frequency acoustic energy harvesting prototype for industrial regions and the Dhaka metro train was effectively developed for residential or commercial areas with heavy noise pollution. With its massive array of barriers, the suggested system offers a workable solution for low-frequency sound absorption and energy production for low-power consumers, including industrial lights, automotive lights, and low-power electronic gadgets.

While there can be different designs, orientations, and numbers of films used to develop energy from low-frequency acoustic vibrations, this study targeted to find out an optimum solution for effective energy harvesting while keeping the cost to an affordable standard.

This technique may be used by power plants and enterprises that generate a lot of noise to conserve electricity and lower the noise level, benefiting nearby inhabitants and workers. However, there are always scopes for betterment.

Chapter Six

References

1. Patwari, A. U., Shan, A. N. M. N. U., Mostafa, M. Z., & Shohan, M. I. U. (2022). *Experimental Investigation on Acoustic Energy Conversion Using Single and Double PZT Film by Modified Resonator*. In Springer eBooks (pp. 86–95). https://doi.org/10.1007/978-981-16-8954-3_9
2. *Helmholtz Resonator—Wolfram Language Documentation*. (n.d.). <https://reference.wolfram.com/language/PDEModels/tutorial/Acoustics/ModelCollection/HelmholtzResonator.html>
3. Lan, J., Li, Y., Yu, H., Li, B., & Liu, X. (2017). Nonlinear effects in acoustic metamaterial based on a cylindrical pipe with ordered Helmholtz resonators. *Physics Letters*, 381(13), 1111–1117. <https://doi.org/10.1016/j.physleta.2017.01.036>
4. Chorsi, M. T., Curry, E. J., Chorsi, H. T., Das, R., Baroody, J., Purohit, P. K., Ilieş, H. T., & Nguyen, T. N. (2019). Piezoelectric Biomaterials for Sensors and Actuators. *Advanced Materials*, 31(1), 1802084. <https://doi.org/10.1002/adma.201802084>
5. Lancaster, D. (2022). 4 common types of piezoelectric sensor. *Electronic Guidebook*. <https://electronicguidebook.com/4-common-types-of-piezoelectric-sensor>
6. *PZT thin-film sensors and actuators*. (2017, January 24). Mechanical Engineering. https://www.me.washington.edu/research/faculty/ishen/actuators_sensors
7. Lu, Z., Dorantes-Gonzalez, D. J., Chen, K., Yang, F., Jin, B., Li, Y., Chen, Z., & Hu, X. (2012). A Four-Quadrant PVDF Transducer for Surface Acoustic Wave Detection. *Sensors*, 12(8), 10500–10510. <https://doi.org/10.3390/s120810500>
8. Inc, E. (n.d.). *Piezoelectric Sensor: types, working principle, and applications / Easybom*. Easybom Inc All Rights Reserved. <https://www.easybom.com/blog/a/piezoelectric-sensor>
9. Zhang, Z., Zhang, X., Chen, W., Rasim, Y., Salman, W., Pan, H., Yuan, Y., & Wang, C. (2016). A high-efficiency energy regenerative shock absorber using supercapacitors for renewable energy applications in range extended electric vehicle. *Applied Energy*, 178, 177–188. <https://doi.org/10.1016/j.apenergy.2016.06.054>
10. Wang, H., Jasim, A. F., & Chen, X. (2018). Energy harvesting technologies in roadway and bridge for different applications – A comprehensive review. *Applied Energy*, 212, 1083–1094. <https://doi.org/10.1016/j.apenergy.2017.12.125>

11. Zhang, X., Zhang, Z., Pan, H., Salman, W., Yuan, Y., & Liu, Y. (2016). A portable high-efficiency electromagnetic energy harvesting system using supercapacitors for renewable energy applications in railroads. *Energy Conversion and Management*, *118*, 287–294. <https://doi.org/10.1016/j.enconman.2016.04.012>
12. Feenstra, J., Granstrom, J., & Sodano, H. A. (2008). Energy harvesting through a backpack employing a mechanically amplified piezoelectric stack. *Mechanical Systems and Signal Processing*, *22*(3), 721–734. <https://doi.org/10.1016/j.ymssp.2007.09.015>
13. Abdelmoula, H., Sharpes, N., Abdelkefi, A., Lee, H., & Priya, S. (2017). Low-frequency Zigzag energy harvesters operating in torsion-dominant mode. *Applied Energy*, *204*, 413–419. <https://doi.org/10.1016/j.apenergy.2017.07.044>
14. Zorlu, O., Topal, E. T., & Kulah, H. (2011). A Vibration-Based Electromagnetic Energy Harvester Using Mechanical Frequency Up-Conversion Method. *IEEE Sensors Journal*, *11*(2), 481–488. <https://doi.org/10.1109/jsen.2010.2059007>
15. Anton, S. R., & Sodano, H. A. (2007). A review of power harvesting using piezoelectric materials (2003–2006). *Smart Materials and Structures*, *16*(3), R1–R21. <https://doi.org/10.1088/0964-1726/16/3/r01>
16. Hansen, B., Liu, Y., Yang, R., & Wang, Z. L. (2010). Hybrid Nanogenerator for Concurrently Harvesting Biomechanical and Biochemical Energy. *ACS Nano*, *4*(7), 3647–3652. <https://doi.org/10.1021/nn100845b>
17. Ovejas, V. J., & Cuadras, A. (2011). Multimodal piezoelectric wind energy harvesters. *Smart Materials and Structures*, *20*(8), 085030. <https://doi.org/10.1088/0964-1726/20/8/085030>
18. Fondevilla, N., Serre, C., Pérez-Rodríguez, A., Acero, M., Cabruja, E., Campanella, H., & Esteve, J. (2011). *Electromagnetic harvester device for scavenging ambient mechanical energy with slow, variable, and randomness nature*. <https://doi.org/10.1109/powereng.2011.6036432>
19. Kim, S., Ji, C., Galle, P., Herrault, F., Wu, X., Lee, J. Y., Choi, C., & Allen, M. G. (2009). An electromagnetic energy scavenger from direct airflow. *Journal of Micromechanics and Microengineering*, *19*(9), 094010. <https://doi.org/10.1088/0960-1317/19/9/094010>
20. Lallart, M., Guyomar, D., Richard, C., & Petit, L. (2010). Nonlinear optimization of acoustic energy harvesting using piezoelectric devices. *Journal of the Acoustical Society of America*, *128*(5), 2739–2748. <https://doi.org/10.1121/1.3290979>
21. Guan, M., & Liao, W. (2016). Design and analysis of a piezoelectric energy harvester for rotational motion system. *Energy Conversion and Management*, *111*, 239–244. <https://doi.org/10.1016/j.enconman.2015.12.061>

22. Horowitz, S. B., Sheplak, M., Cattafesta, L. N., & Nishida, T. (2006). A MEMS acoustic energy harvester. *Journal of Micromechanics and Microengineering*, 16(9), S174–S181. <https://doi.org/10.1088/0960-1317/16/9/s02>
23. Yuan, M., Cao, Z., Luo, J., Zhang, J., & Chang, C. Y. (2017). An efficient low-frequency acoustic energy harvester. *Sensors and Actuators A-physical*, 264, 84–89. <https://doi.org/10.1016/j.sna.2017.07.051>
24. Wang, Y., Zhu, X., Zhang, T., Bano, S., Pan, H., Qi, L., Zhang, Z., & Yuan, Y. (2018). A renewable low-frequency acoustic energy harvesting noise barrier for high-speed railways using a Helmholtz resonator and a PVDF film. *Applied Energy*, 230, 52–61. <https://doi.org/10.1016/j.apenergy.2018.08.080>
25. Wu, L., Chen, L., & Liu, C. (2009b). Acoustic energy harvesting using resonant cavity of a sonic crystal. *Applied Physics Letters*, 95(1), 013506. <https://doi.org/10.1063/1.3176019>
26. Yuan, M., Cao, Z., Luo, J., & Chou, X. (2019). Recent Developments of Acoustic Energy Harvesting: A Review. *Micromachines*, 10(1), 48. <https://doi.org/10.3390/mi10010048>
27. Pillai, M. A., & Deenadayalan, E. (2014). A review of acoustic energy harvesting. *International Journal of Precision Engineering and Manufacturing*, 15(5), 949–965. <https://doi.org/10.1007/s12541-014-0422-x>
28. Williams, C., & Yates, R. (1996). Analysis of a micro-electric generator for microsystems. *Sensors and Actuators A-physical*, 52(1–3), 8–11. [https://doi.org/10.1016/0924-4247\(96\)80118-x](https://doi.org/10.1016/0924-4247(96)80118-x)
29. Khan, F. U., & Izhar. (2013). *Electromagnetic-based acoustic energy harvester*. <https://doi.org/10.1109/inmic.2013.6731337>
30. Glynne-Jones, P., Tudor, M., Beeby, S., & White, N. J. (2004). An electromagnetic, vibration-powered generator for intelligent sensor systems. *Sensors and Actuators A-physical*, 110(1–3), 344–349. <https://doi.org/10.1016/j.sna.2003.09.045>
31. Ferrari, M., Ferrari, V., Guizzetti, M., Marioli, D., & Taroni, A. (2008). Piezoelectric multi-frequency energy converter for power harvesting in autonomous microsystems. *Sensors and Actuators A-physical*, 142(1), 329–335. <https://doi.org/10.1016/j.sna.2007.07.004>
32. Vatansever, D., Hadimani, R. L., Shah, T., & Siores, E. (2011). An investigation of energy harvesting from renewable sources with PVDF and PZT. *Smart Materials and Structures*, 20(5), 055019. <https://doi.org/10.1088/0964-1726/20/5/055019>
33. Li, B., & You, J. S. (2011). Harvesting ambient acoustic energy using acoustic resonators. *Journal of the Acoustical Society of America*, 129(4), 2449. <https://doi.org/10.1121/1.3588028>

34. Jo, S. J., Kim, M. S., & Kim, Y. (2012). A resonant frequency switching scheme of a cantilever based on polyvinylidene fluoride for vibration energy harvesting. *Smart Materials and Structures*, 21(1), 015007. <https://doi.org/10.1088/0964-1726/21/1/015007>
35. Orrego, S., Shoele, K., Ruas, A., Doran, K., Caggiano, B., Mittal, R., & Kang, S. K. (2017). Harvesting ambient wind energy with an inverted piezoelectric flag. *Applied Energy*, 194, 212–222. <https://doi.org/10.1016/j.apenergy.2017.03.016>
36. Vocca, H., Neri, I., Travasso, F., & Gammaitoni, L. (2012). Kinetic energy harvesting with bistable oscillators. *Applied Energy*, 97, 771–776. <https://doi.org/10.1016/j.apenergy.2011.12.087>
37. Li, B., You, J. S., & Kim, Y. (2013b). Low frequency acoustic energy harvesting using PZT piezoelectric plates in a straight tube resonator. *Smart Materials and Structures*, 22(5), 055013. <https://doi.org/10.1088/0964-1726/22/5/055013>
38. Li, B., Laviage, A. J., You, J. S., & Kim, Y. (2013). Harvesting low-frequency acoustic energy using quarter-wavelength straight-tube acoustic resonator. *Applied Acoustics*, 74(11), 1271–1278. <https://doi.org/10.1016/j.apacoust.2013.04.015>
39. Roshani, H., Dessouky, S., Montoya, A., & Papagiannakis, A. T. (2016). Energy harvesting from asphalt pavement roadways vehicle-induced stresses: A feasibility study. *Applied Energy*, 182, 210–218. <https://doi.org/10.1016/j.apenergy.2016.08.116>
40. Zhao, H., Xiao, X., Xu, P., Zhao, T., Song, L., Pan, X., Mi, J., Xu, M., & Wang, Z. L. (2019). Dual-Tube Helmholtz Resonator-Based Triboelectric Nanogenerator for Highly Efficient Harvesting of Acoustic Energy. *Advanced Energy Materials*, 9(46), 1902824. <https://doi.org/10.1002/aenm.201902824>
41. Liu, F., Horowitz, S., Nishida, T., Cattafesta, L. N., & Sheplak, M. (2007). A multiple degree of freedom electro-mechanical Helmholtz resonator. *Journal of the Acoustical Society of America*, 122(1), 291–301. <https://doi.org/10.1121/1.2735116>
42. Liu, F., Phipps, A., Horowitz, S., Ngo, K. D. T., Cattafesta, L. N., Nishida, T., & Sheplak, M. (2008). Acoustic energy harvesting using an electro-mechanical Helmholtz resonator. *Journal of the Acoustical Society of America*, 123(4), 1983–1990. <https://doi.org/10.1121/1.2839000>
43. Zhou, Z., & Zhu, P. (2017). Harvesting acoustic energy by coherence resonance of a bi-stable piezoelectric harvester. *Energy*, 126, 527–534. <https://doi.org/10.1016/j.energy.2017.03.062>
44. Noh, S., Lee, H., & Choi, B. (2013). A study on the acoustic energy harvesting with Helmholtz resonator and piezoelectric cantilevers. *International Journal of Precision Engineering and Manufacturing*, 14(9), 1629–1635. <https://doi.org/10.1007/s12541-013-0220-x>

45. Zhang, Z., Zhang, X., Rasim, Y., Wang, C., Du, B., & Yuan, Y. (2016). Design, modelling and practical tests on a high-voltage kinetic energy harvesting (EH) system for a renewable road tunnel based on linear alternators. *Applied Energy*, *164*, 152–161. <https://doi.org/10.1016/j.apenergy.2015.11.096>
46. Lupea, I. (2012). Considerations on the Helmholtz resonator simulation and experiment. *Proceedings of the Romanian Academy, Series A-Mathematics Physics Technical Sciences Information Science*, *13*(2), 118-124.
47. Roundy, S., & Wright, P. K. (2004). A piezoelectric vibration based generator for wireless electronics. *Smart Materials and Structures*, *13*(5), 1131–1142. <https://doi.org/10.1088/0964-1726/13/5/018>
48. Hu, Z., Yang, C., & Cheng, L. (2018). Acoustic resonator tuning strategies for the narrowband noise control in an enclosure. *Applied Acoustics*, *134*, 88–96. <https://doi.org/10.1016/j.apacoust.2018.01.013>
49. Smits, J. M. M., & Ballato, A. (1994). Dynamic admittance matrix of piezoelectric cantilever bimorphs. *Journal of Microelectromechanical Systems*, *3*(3), 105–112. <https://doi.org/10.1109/84.311560>
50. Abrams, Z. R., Niv, A., & Zhang, X. (2011). Solar energy enhancement using down-converting particles: A rigorous approach. *Journal of Applied Physics*, *109*(11), 114905. <https://doi.org/10.1063/1.3592297>
51. Meirovitch, L. (1975). *Elements of vibration analysis*. <https://ci.nii.ac.jp/ncid/BA26927517>